

Solving Crystal Structures by Carrying Out the Calculation of the Single-Atom R1 Method in a Lottery Mode

Authors

Xiaodong Zhang^{a*}

^aChemistry Department, Tulane University, 6400 Freret Street, New Orleans, Louisiana, 70118, United States

Correspondence email: xzhang2@tulane.edu

Synopsis A lottery scheme of carrying out the single-atom R1 (sR1) calculation has been designed for solving crystal structures.

Abstract As originally designed [Zhang & Donahue (2024), *Acta Cryst. A* **80**, 237-248.], after one cycle of calculation, the single-atom R1 (sR1) method required a user to intelligently determine a partial structure to start the next cycle. In this paper, a lottery scheme has been designed to randomly split a parent model into two child models. This allows the calculation to be carried out in a care-free manner. By chance, one child model may have higher amounts of “good” atoms than the parent model. Thus, its expansion in the next cycle favors an improved model. These “lucky” results are carried onto the next cycles, while “unlucky” results in which no improvements occur are discarded. Furthermore, unchanged models are carried onto the next cycles in those “unlucky” occasions. On average a child model has the same fraction of “good” atoms as the parent. Only a substantial statistical fluctuation results in appreciable deviation. This lottery scheme works because such fluctuations do happen. Indeed, test applications with the computing power accessible by the author have demonstrated that the designed scheme can drive an sR1 calculation to or close to reaching a correct structure solution.

Keywords: single-atom R1; lottery scheme; statistical fluctuation; structure solution

1. Introduction

In X-ray crystallography, many methods for solving crystal structures rely on phasing (Giacovazzo, 2014). The modern driving force behind many phasing methods is a dual space recycling process, utilizing reciprocal space phase refinement and/or real space electron density modifications (Weeks *et al.*, 1993; Miller *et al.*, 1993; DeTitta *et al.*, 1994). One way of phasing in macromolecular crystallography is the molecular replacement (MR) method (Rossmann & Blow, 1962; Rossmann *et al.*, 1964; Crowther, 1972; Rossmann, 1972, 1990; Bricogne, 1992; Read, 2001; McCoy, 2004; Read & McCoy, 2016; McCoy *et al.*, 2017; Caliandro *et al.*, 2009; Burla *et al.*, 2020). The key step of an MR calculation is using a model-searching technique to orient and translationally position a known model (or models) in an unknown structure. Originally, Patterson targets (rotation function, Rossmann & Blow, 1962; translation function, Rossmann *et al.*, 1964) were used for this task. Currently, the log-likelihood-gain on intensities (LLGI), which is the sum of log-likelihoods for individual reflections minus the log-likelihood of an uninformative model (McCoy *et al.*, 2007; Read & McCoy, 2016), is used as it is regarded as the most sensitive target for model searching. In early days of the MR method, the traditional R1 was occasionally used as a target with some success in translational search (Eventoff *et al.*, 1975; Bott & Sarma, 1976). Today, the traditional R1 is regarded as a poor target for model searching (McCoy, 2017). But a recent paper (Zhang & Donahue, 2024) yielded rather surprising results. In that publication, an approximate R1, called the single-atom R1 (sR1), was used to solve small molecule crystal structures by locating missing atoms of a structure one at a time. Essentially, the sR1 was used as a target for single atom search, and it was very successful in this regard. In fact, the whole structure of each tested case was directly solved by the sR1 method, with no need of phasing.

The calculation of the sR1 method is carried out in cycles, in which each cycle expands a starting partial model into a tentative full model (Zhang & Donahue, 2024). As originally designed, a transition from one cycle to the next requires a user to intelligently determine the next starting partial model. This is done either by selecting recognizable fragments, or by manually deleting ghost atoms. The aim of this paper is to relax this requirement by designing a lottery scheme that automatically generates starting partial models. Such a scheme has been designed with its effectiveness verified by test calculations. The paper will also discuss implications of this novel design.

2. Recap of the nature of the approximation in defining the single-atom R1 (sR1)

The sR1 is derived from the traditional R1 by approximation. Readers should refer to the previous paper (Zhang & Donahue, 2024) for the explicit formulas. However, it is instructive to recap the main ideas leading to this approximation. The goal is to solve a structure with N atoms in its unit cell. The starting point is a partial model with atoms 1 to $i - 1$ already being located. The coordinates of the atoms from i to N are still undetermined. Usually, it is a daunting task to handle all these

undetermined atoms together. It is much easier to handle a single atom or a group of atoms (for example, a fragment with a known structure) rather than handling every undetermined atom. Let atoms i to j be the single atom (if $i = j$) or the group of atoms (if $i < j$) that one wishes to focus on. The atoms from $j + 1$ to N are the other remaining undetermined atoms, whose fractional coordinates one wishes to get rid of from the formula of the R1. Thus, an approximation is made by deleting terms containing these coordinates from the R1 formula. However, the resulting approximate R1 is not completely unrelated to these other undetermined atoms. It is no longer related to the coordinates of these atoms, but it is still related to their atomic scattering factors through a term of the sum of the square of the atomic scattering factors of these atoms. This term is retained for the purpose of calculating the approximate R1 as accurately as possible. This approximate R1 is called the single-atom R1 (sR1) if $i = j$, or the partial-structure R1 (pR1) if $i < j$. In the sR1, atoms 1 to $j - 1$ are the ones that have already been located; atom j is the only single undetermined atom whose coordinates one wishes to determine. In the pR1, atoms 1 to $i - 1$ are the ones already being located, and atoms i to j belong to a fragment whose orientation and translational position one wishes to determine.

The atomic scattering factors, which are calculated with an isotropic displacement parameter $U=0 \text{ \AA}^2$, are used for calculating the approximate R1. These atomic scattering factors are related to the underlying atomic electron density of spherical shapes. One intuition for understanding the sR1 method is to notice that the centers of atomic electron density spheres of atoms 1 to $j - 1$ are fixed in the unit cell. On the other hand, the center of atom j is moving around in the cell, and one is trying to see which j location can best account the diffraction effects. However, one should realize that because the dependence of the sR1 on the coordinates of atoms $j + 1$ to N has been removed while the dependence on the atomic scattering factors of these atoms are partially retained, a correspondence to the spheres of the atomic electron density for these atoms is lost. This subtlety, in addition to the fact that the sR1 method does not explicitly calculate an electron density, makes the method not even implicitly related to an electron density of some partial structure.

3. Improvements on the implementation of the sR1 method

The basic implementation of the sR1 method remains the same as reported previously (Zhang & Donahue, 2024). However, two improvements have been made. First, instead of directly feeding raw reflection intensities to the calculation, sharpened intensities are used. A sharpened intensity is calculated as the product of multiplying a raw intensity $F_0^2(hkl)$ with $\exp(2Bs^2)$, where $s = \sin\theta/\lambda$. The parameter B is determined by the Wilson method. Implementation of the Wilson method is given in the supporting information. Second, the precision of the coordinates of the single atoms are refined to 0.2 \AA , instead of previous 0.001 \AA . This cuts the calculation time while still yielding good solutions.

4. Designing a lottery scheme for transition from one sR1 calculation cycle to the next

The idea of playing lottery in the sR1 calculation was inspired by one published work (Burla *et al.*, 2018). In that work, a diagonal least-squares technique was used to produce *ab initio* phasing of small molecules. During the calculation, poorly located atoms were identified and replaced with new atoms that were randomly positioned.

Each cycle of an sR1 calculation expands a starting partial model into a tentative full model. To start the next cycle, a new starting partial model needs to be determined. In the original design (Zhang & Donahue, 2024), a user determines this new starting partial model either by selecting a recognizable fragment (or fragments) or by deleting ghost atoms from the tentative full model. Therefore, that design can be regarded as performing the calculation in an intelligent mode.

Ideally, the new starting partial model should only include those atoms that have been correctly located. The question is how to identify these correctly located atoms. Or, conversely, how does one identify those more-likely poorly located atoms? Burla *et al.* (2018) were able to identify poorly located atoms by checking their anisotropic displacement parameters in a diagonal least-squares calculation. But inserting a least-squares calculation slows down the sR1 method. A better alternative is to borrow another idea from another published work (Kinneking & de Graaff, 1984) in which some R1 calculation was used to identify poorly located atoms. In the sR1 calculation, when a new atom is added to the growing model, the approximate R1 usually drops. Intuitively, how much the approximate R1 drops measures how well the newly added atom contributes to accounting the diffraction effects. Reciprocally, if the addition of an atom causes the approximate R1 to rise, it is very likely this atom is incorrectly positioned. In fact, this has been verified by applying the sR1 method to about 200 datasets (a summary of these test calculations is given in the supporting information). Often, such atoms are ghost atoms. Only very rarely does adding correct atoms make the approximate R1 rise. Therefore, in the new calculation scheme, all the atoms that cause the approximate R1 to rise will be excluded when generating a new starting partial model. It should be acknowledged that a reviewer compared this process of rejecting atoms to iterative peaklist optimization where peaks are eliminated one by one to maximize CC (Sheldrick & Gould, 1995).

After excluding these very likely bad atoms, the remaining atoms are not all correctly located. But trying to figure out further which atoms are more likely correctly located is difficult. Therefore, a lottery must be played. A parent model is formed with the remaining atoms and is randomly split into two child models. On average a child model contains the same fraction of “good” atoms as the parent. Only a substantial statistical fluctuation can noticeably swing its content away from this average. Though statistical fluctuation happens in any system size, large fluctuations (as scaled by the size of the system) are more likely in small size systems. Accordingly, one child model is designed to be small (with about 1 to 20 atoms) on purpose so that it becomes variable to chance. When a fluctuation

causes the small child model to contain nearly all “bad” atoms, its sibling (a large child model) will have slightly more “good” atoms than the parent, and an expansion from this sibling likely leads to a slight improvement on the tentative full model. On the other hand, when a fluctuation causes the small child model to contain nearly all “good” atoms and the parent model is still poorly determined, an expansion from this good small child model may greatly improve the tentative full model. These expectations have been verified by test calculations (see section 6).

With all above considerations in mind, the following scheme of splitting a parent model has been designed. Let N be the number of atoms in the parent model. Calculate $p_1 = 20/N$. If $p_1 > 0.5$, take $p_1 = 0.5$. Generate a random number p_0 that is uniformly distributed from 0 to p_1 . For each atom in the parent model, generate a random number p that is uniformly distributed from 0 to 1. If $p > p_0$, assign this atom to child model 1; otherwise, assign it to child model 2. If either of the child models happens to be empty, try another split.

Figure 1 shows a general flow chart of an sR1 calculation in lottery mode. The whole calculation starts from an initial starting model, which is either a single atom or one/two/a few fragments of a known structure oriented and translationally positioned by the partial-structure R1 (pR1) method (Zhang & Donahue, 2024). This starting model is expanded to model 0 by one cycle of the sR1 calculation. After deleting the likely bad atoms (namely those when introduced caused the approximate R1 to rise) model 0 is split into child models 1 and 2 by the above-mentioned scheme. Expand child model 1 into model 1 by one cycle of the sR1 calculation. If model 1 is an improvement over model 0 (see the next paragraph on how this comparison is made), take model 1 as the new model 0 and move on to the next lottery cycle. Otherwise, expand child model 2 into model 2 by one cycle of the sR1 calculation. If model 2 is an improvement over model 0, take model 2 as the new model 0 and move on to the next lottery cycle. Otherwise, start the next lottery cycle with the unchanged model 0. Note that the lottery cycles go indefinitely. A user can check the improvement of model 0 from time to time and later decide when to terminate the calculation.

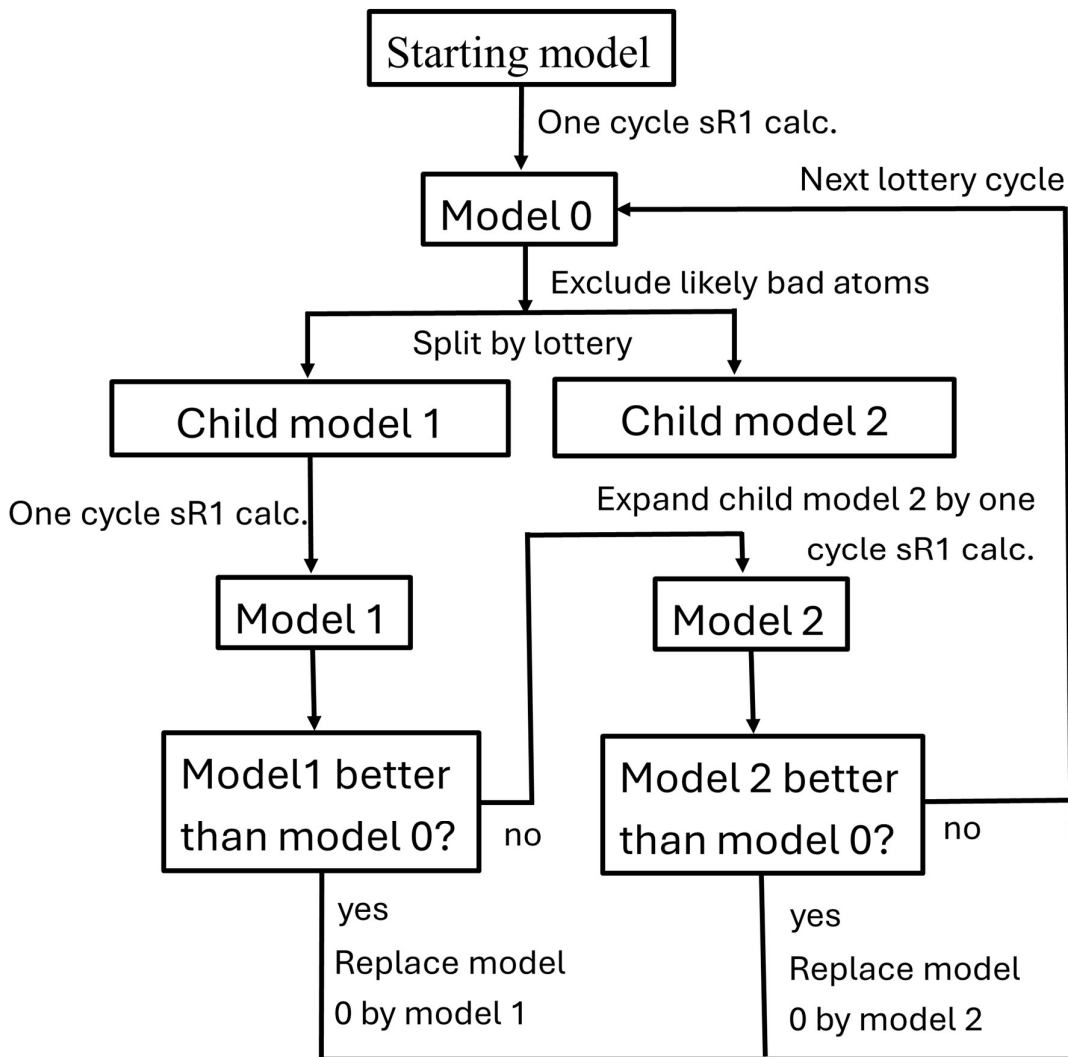


Figure 1 A general flow chart of an sR1 calculation in a lottery mode.

One thing remains unclear though. How can it be seen whether model 1 (or 2) is an improvement over model 0? When a model grows by adding atoms one by one, the approximate R1 usually drops, but sometimes it increases. By intuition, the minimum approximate R1 ever reached is a good measure of how good the resulting model (after excluding the likely bad atoms as described above) is. This standard has been adopted for comparing models. If the minimum approximate R1 that has been reached when building model 1 is lower than that when building model 0, model 1 is an improvement over model 0. The same rule is applied for comparing model 2 with model 0.

5. Test calculations

The crystallographic information of the samples used in the test calculations is listed in Table 1. The samples will be referred to by their sample numbers.

Table 1 Crystallographic information of the samples used in the test calculations

Sample	Formula (excluding H)	Z	non- hydrogen atoms in cell	Resolution (Å)	a(Å)	b(Å)	c(Å)	α (°)	β (°)	γ (°)	space group
1	FN ₂ C ₁₃	8	128	12.1 – 0.79	8.45	9.93	24.20	90.00	90.00	90.00	Pbca
2	O ₂ C ₂₉	8	248	10.7 – 1.00	44.17	10.73	8.93	90.00	90.00	90.00	Pbcn
3	F ₂ O ₄ N ₂ C ₅₂	4	240	24.2 – 0.90	12.27	24.23	15.42	90.00	96.94	90.00	P2 ₁ /c
4	PdS ₆ P ₄ C ₆₈	4	316	10.5 – 0.85	23.32	14.45	22.39	90.00	115.22	90.00	P2 ₁ /c

In the following each resulting model was compared to a “correct” model. Here is how such a “correct” model was obtained. A structure was “solved” by the program *SHELXT* (Sheldrick, 2015a). After going through “refinement” with the program *SHELXL* (Sheldrick, 2015b) and deleting H atoms, the structure was expanded to the P1 space group. This expanded structure is the “correct” model. A comparison between a resulting model with a “correct” model helped to verify that the sR1 method reached approximately the same model as the program *SHELXT* did.

5.1. One typical example

Typically, the sR1 method can solve a small molecule structure by starting from a single atom (Zhang & Donahue, 2024). Sample 1 is one such typical example. As seen in Table 1, sample 1 has 128 non-hydrogen atoms in its unit cell. As shown in figure 2, when running in lottery mode, the sR1 calculation can reach a final model of sample 1 by the end of lottery cycle 33. This final model, when compared to the correct model, has all 128 atoms being located within 0.5 Å of their corresponding correct locations.

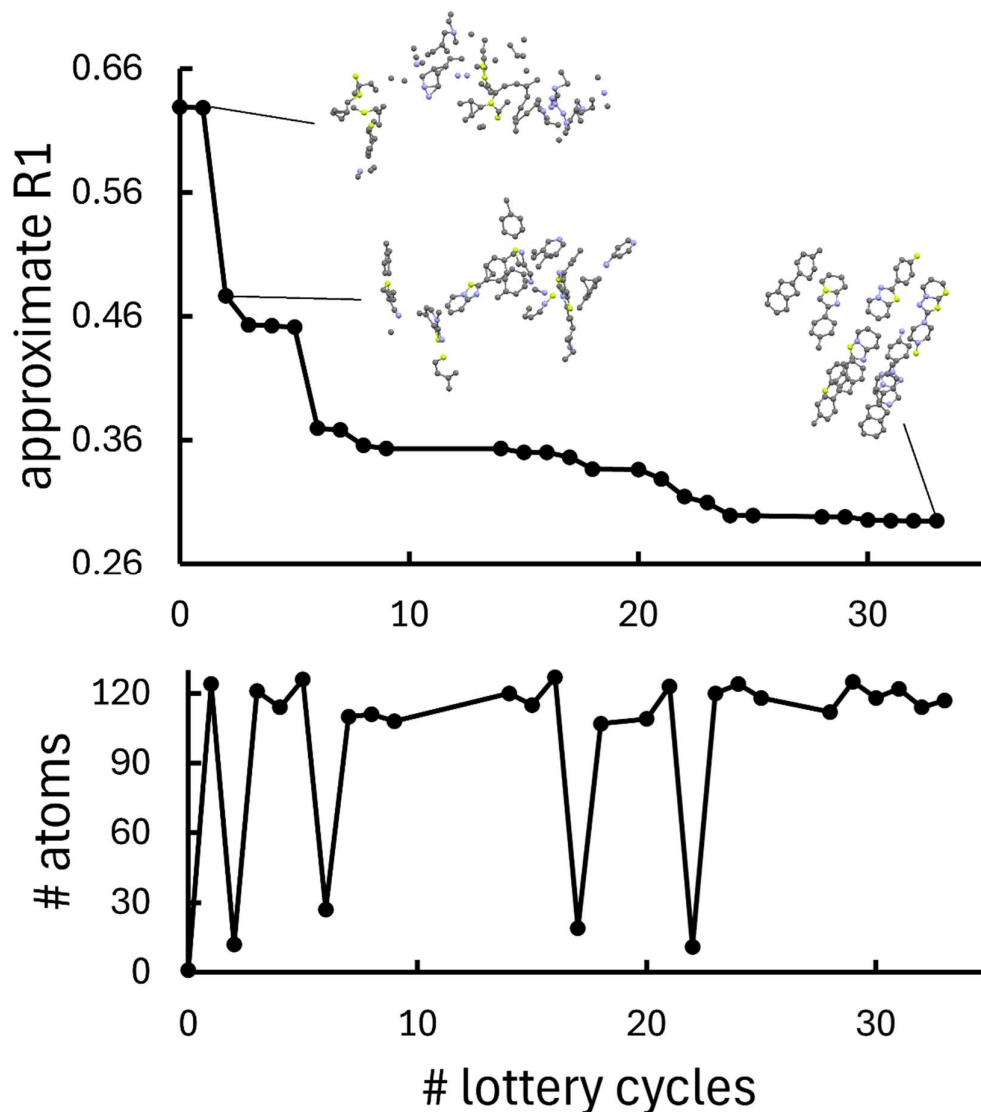


Figure 2 Solving the structure of sample 1 by running the sR1 calculation in lottery mode, starting from a single F atom at (0.3, 0.3, 0.3). The top chart shows how the minimum approximate R1 that has been reached in each lottery cycle drops when the calculation proceeds. The bottom chart shows the size of the starting partial model of each lottery cycle. The inserts show the model structures at the end of cycles 1, 2, and 33, respectively.

5.2. Another typical example but with more atoms

Sample 2 is another typical example for which the sR1 calculation can start from a single atom. The structure of sample 2 is much larger than that of sample 1. As seen in Table 1, sample 2 has 248 non-hydrogen atoms in its unit cell compared to sample 1's 128. Figure 3 shows that, by the end of lottery cycle 48, the result of solving sample 2 is close to complete. Compared with the correct model, this

result has 239 atoms located within 0.5 Å of their corresponding correct locations, with only 9 atoms being misplaced.

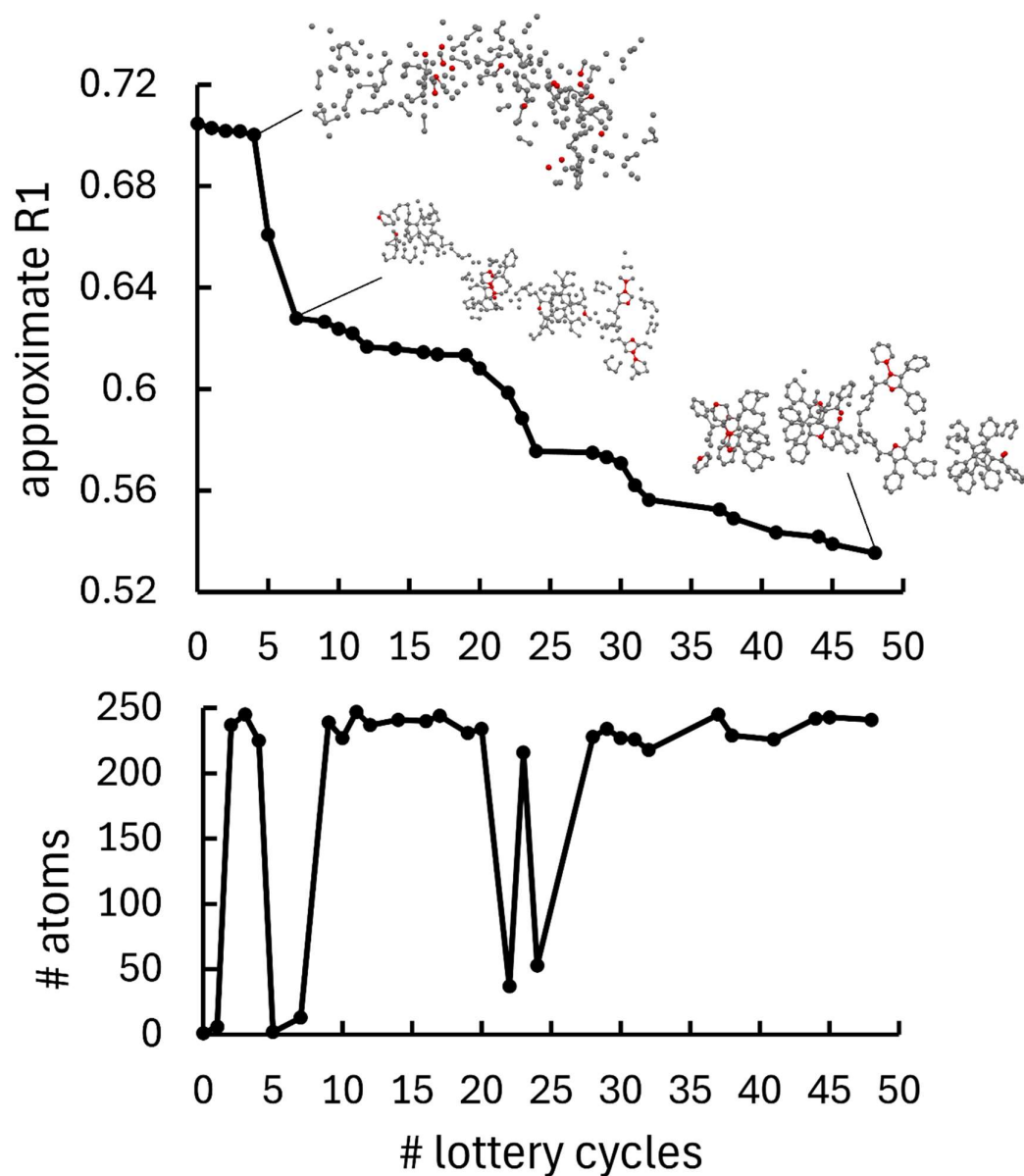


Figure 3 Solving the structure of sample 2 by running the sR1 calculation in lottery mode, starting from a single O atom at (0.3, 0.3, 0.3). The top chart shows how the minimum approximate R1 that has been reached in each lottery cycle drops when the calculation proceeds. The bottom chart shows the size of the starting partial model of each lottery cycle. The inserts show the model structures at the end of cycles 4, 7, and 48, respectively.

5.3. An example of a difficult case

The author has tested the sR1 method over around 200 datasets (see the list within supporting information). For most cases the calculation is straightforward by starting from a single atom at (0.3, 0.3, 0.3). For some of these straightforward cases the structure is revealed by one sR1 cycle, but most of these cases require multiple cycles with a user's guidance of selecting fragments and/or deleting ghost atoms. Then, there are a few difficult cases in which a single sR1 cycle starting from a single atom at (0.3, 0.3, 0.3) does not reveal any recognizable fragments. For these difficult cases the sR1 calculation needs to be jumpstarted by using the partial-structure R1 (pR1) method to orient and translationally position one/two/a few fragments of a known structure (Zhang & Donahue, 2024). Sample 3 is one of these difficult cases. Figure 4 shows the general steps of solving the structure of sample 3. The first step is to use the pR1 method to orient and translationally position two benzene rings. The second step is to perform the lottery cycles by starting from the partial model of the two benzene rings. Figure 5 shows the details of this step. The result of these lottery cycles contains some ghost atoms. However, it should not be expected that the sR1 method can clean out all these ghost atoms as some of these "ghost" atoms are real – they arise from other unknown diffraction centers, disordered solvent, etc. The main goal of solving a structure is to reveal the primary structure. So, these "ghost" atoms are deleted. The third step uses a simple trick to discover the missing atoms of the primary structure. This simple trick can be called the bond length guided sR1 method. Though the author came across this simple idea with no knowledge of the existence of other programs, as one reviewer has pointed out, it should be acknowledged that similar ideas have been well exploited in other programs, including *ARPWarp* (Lamzin *et al.*, 2012), *Coot* (Emsley *et al.*, 2010) and *PHENIX AutoBuild* wizard (Terwilliger *et al.*, 2008). The underlying principle of this idea is to let A be an atom that has already been located and Q be an undetermined atom which is expected to bond to atom A with an approximate bond length r . The approximate C-C bond length 1.39 Å was used in this work. A grid has been set up within the unit cell with step size 0.4 Å. To coarsely locate atom Q, only the grid points that are located within a spherical shell, which centers at atom A and has radii $r - \Delta r \sim r + \Delta r$, need to be tested. Here, Δr takes the value of either 0.3, or 0.4, or 0.5 Å (in this report, 0.3 Å was used). Other than limiting the initial search range for positioning atom Q, the rest of the bond length guided sR1 calculation is the same as the normal sR1 procedure (Zhang & Donahue, 2024). The third step of figure 4 shows the final model of sample 3 after discovering the missing atoms by the bond length guided sR1 method. Compared with the correct model, this result has all 240 atoms being located within 0.5 Å of their corresponding correct locations, with no atoms being misplaced.

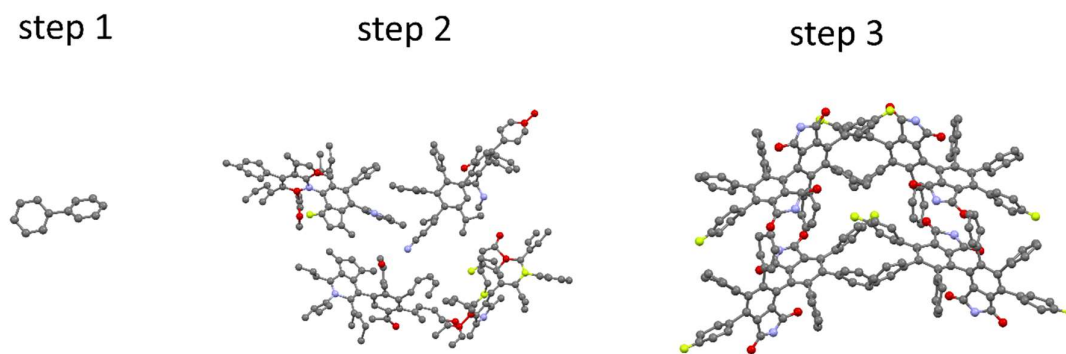


Figure 4 General steps of solving the structure of sample 3. Step 1: the partial model formed by using the pR1 method to orient and translationally position two benzene rings. Step 2: the resulting partial structure after running 36 lottery cycles, starting from the partial structure of the two benzene rings. Note that the ghost atoms are deleted from this resulting partial structure. Step 3: the final model after using the bond length guided sR1 method to add the missing atoms. Note that the atom types have been manually corrected.

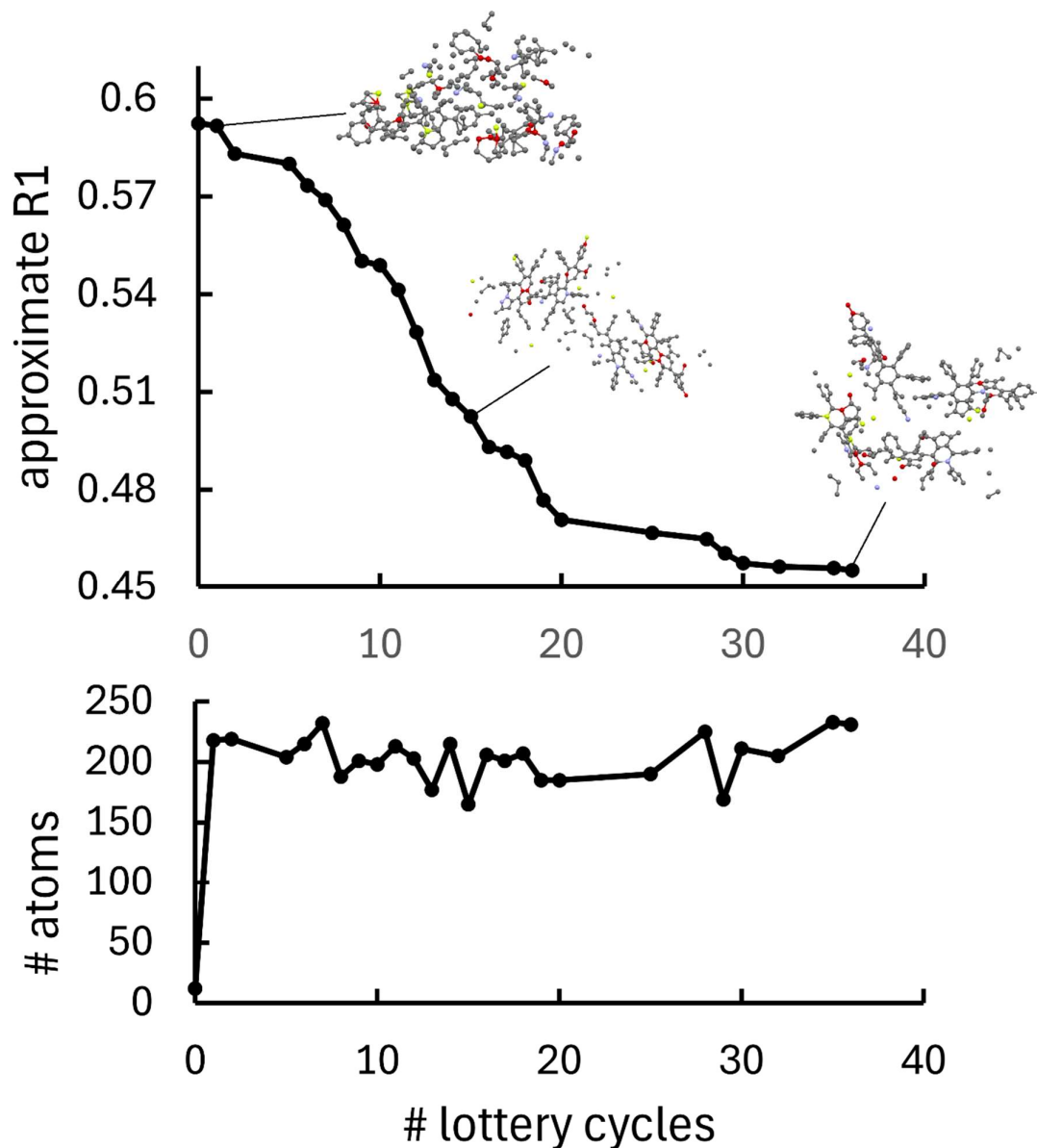


Figure 5 Details of the lottery cycle steps for solving the structure of sample 3, starting from the partial structure of two benzene rings. The top chart shows how the minimum approximate R1 reached in each lottery cycle drops when the calculation proceeds. The bottom chart shows the size of the starting partial model of each lottery cycle. The inserts show the model structures at the end of cycles 1, 15 and 36, respectively.

5.4. A structure containing many heavy atoms

Sample 4 is an example of a structure containing many heavy atoms. The unit cell of this structure contains 4 Pd atoms, 24 S atoms, 16 P atoms, and 272 C atoms (see table 1). There are 44 heavy atoms in this structure. For such a structure, it makes sense to first determine the heavy atom

substructure and then add the light atoms later. Figure 6 shows the general steps of solving the structure of sample 4. The first step is to solve the heavy atom substructure by running the sR1 calculation in lottery mode, starting with a single S atom at (0.3, 0.3, 0.3). The details of the lottery cycles are shown in figure 7. The second step is to add the C atoms by one cycle of the sR1 calculation, starting with the heavy atom substructure that has been discovered in the first step. Step 2 results in some ghost C atoms, which are deleted. In step 3, the missing C atoms are discovered by the bond length guided sR1 method. The final model, when compared to the correct model, has 315 atoms being located within 0.5 Å of their corresponding correct locations, with only one C atom being misplaced.

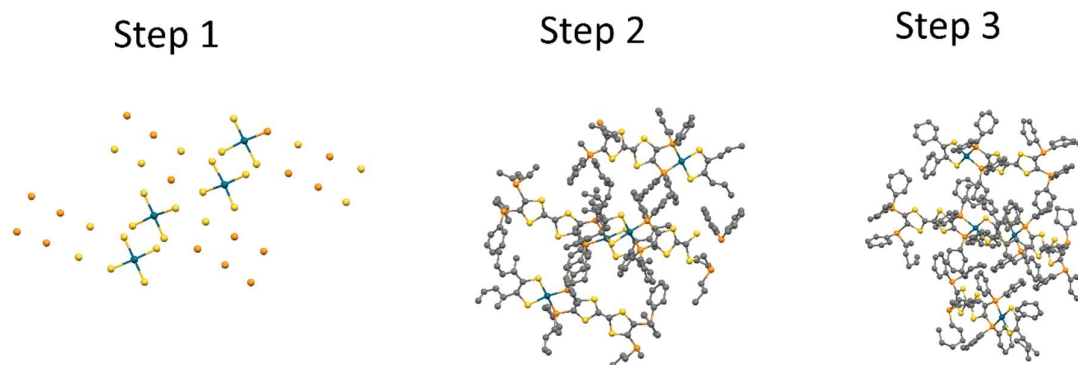


Figure 6 General steps of solving the structure of sample 4. Step 1: the heavy atom substructure discovered by running 6 lottery cycles of the sR1 calculation. Step 2: the resulting partial structure after running one cycle sR1 calculation, starting from the heavy atom substructure. Note that the ghost atoms are deleted from this partial structure. Step 3: the final model after using the bond length guided sR1 method to add the missing C atoms.

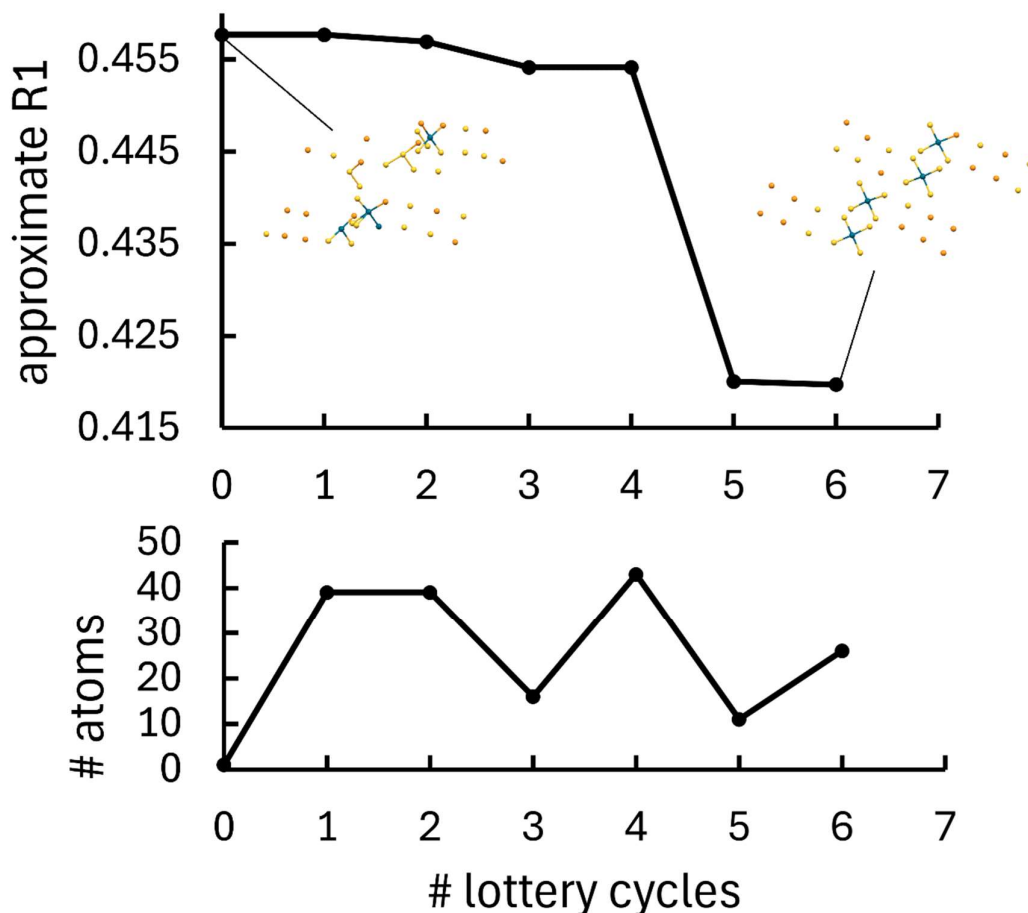


Figure 7 Details of the lottery cycle steps for determining the heavy atom substructure of sample 4, starting from a single S atom at (0.3, 0.3, 0.3). The top chart shows how the minimum approximate R1 reached in each lottery cycle drops when the calculation proceeds. The bottom chart shows the size of the starting partial model of each lottery cycle. The inserts show the models of the heavy atom substructure at the end of cycles 0 and 6, respectively.

6. Discussions and conclusions

6.1. Success rate of the lottery cycles

Figure 2 shows that for solving the structure of sample 1, a total of 33 lottery cycles have been tried. Among those 33 cycles, 26 led to a drop of the approximate R1 (shown on the charts), while 7 were skipped because of failing to improve the model. So, the success rate of the lottery cycles in this case was 26 over 33. Similarly, the success rate for sample 2 was 28 over 48 (Figure 3), for sample 3 25 over 36 (Figure 5), and for sample 4 6 over 6 (Figure 7). Generally, the success rate was higher than 50%. One reason of this high success rate was that in each lottery cycle there were two child models to try. When one child is “worse” than the parent, the other must be “better” than the parent, and its

expansion likely leads to a success. Another likely reason is that one child model has a small size of 1 to 20 atoms. For a small child model, the chance of large statistical fluctuation is high, making the model either contain nearly all “bad” atoms or nearly all “good” atoms. When the small child model contains nearly all “bad” atoms, its large sibling may lead to a small improvement on the solution. On the other hand, when the small child model contains nearly all “good” atoms, it itself can lead to an improvement. The improvement is either great if the parent model is still poorly determined or slight if the parent model has been well determined (see the next sub-section).

6.2. The contribution of small child models vs that of large child models

As seen in the bottom chart of figure 2, for sample 1, out of the 26 successful lottery cycles, 22 were started with large child models. Only 4 were started with small child models. However, the small child models provided most of the improvement on the solution, namely providing the most drop in the approximate R1 (see top chart of figure 2). Among the four occasions of small child models at cycles 2, 6, 18, and 22, cycles 2 and 6 happened when the parent model was still poorly determined. This subsequently caused the approximate R1 to drop dramatically (see top chart of figure 2). On the other hand, cycles 18 and 22 happened when the parent model was well determined, so only small improvements were made at these cycles. As the inserts in figure 2 indicate, the resulting model at the end of cycle 1 had very few recognizable fragments; however, by the end of cycle 2, many recognizable fragments suddenly appeared. This observation of the small child model initiating successful cycles happening less frequently but contributing greatly on improving the solution is also observed for samples 2 (figure 3) and 4 (figure 7). For sample 3 (figure 5), all 25 successful cycles were initiated by large child models. The reason is simple for this occurrence. The calculation of sample 3 was started with a partial model of two benzene rings that were oriented and translationally positioned by the pR1 method. Therefore, it needed to be extremely lucky for a small child model to beat such a starting partial model where a new rebuild from scratch could be accepted.

A cycle started with a large child model aims at making a small improvement, while a cycle started with a small child model aims at rebuilding the model from scratch. The above observations indicate that when the model is still poorly determined, a rebuild can dramatically improve it. For this reason, small child models are important. Though they less frequently lead to improvement, when they do the effects sometimes can be revolutionary.

6.3. The need of a fast-computing tool

For the difficult case of sample 3, is it possible to start the sR1 calculation with a partial model of a single atom instead of using the pR1 method to put two benzene rings? The answer to this question is “Yes”. Figure 8 shows one successful trial of solving the structure of sample 3 by running the sR1 method in the lottery mode, starting with a single F atom at (0.3, 0.3, 0.3). Figure 8 should be compared with figure 5. It is seen that starting from single F atom needed 243 lottery cycles, while

starting from two benzene rings needed only 36 lottery cycles. The comparison of the actual computing time (running on a Microsoft Surface Pro 7) was about 75 hours for the 243 cycles vs about 7 hours for the 36 lottery cycles. Obviously, neither calculation is practical to perform, especially the one starting with a single atom. However, the sR1 method is well suited for parallel calculation. The values of the approximate R1 at all grid points can be calculated simultaneously. So, the whole sR1 map can be analyzed within a split of a millisecond, and the whole calculation can go extremely fast if sufficient computing power is available. If such fast-computing tools are used, all these calculations can be comfortably performed.

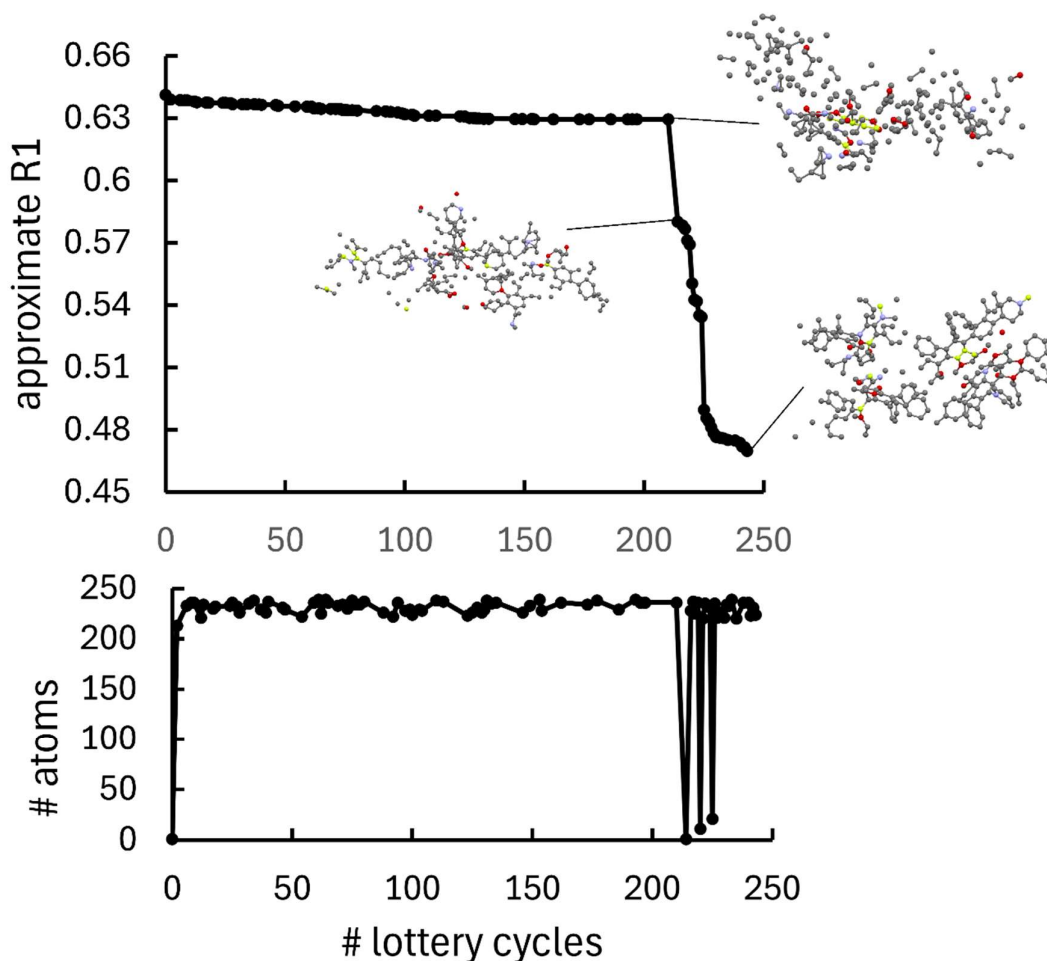


Figure 8 Solving the structure of sample 3 by running the sR1 calculation in lottery mode, starting from a single F atom at (0.3, 0.3, 0.3). The top chart shows how the minimum approximate R1 in each lottery cycle drops when the calculation proceeds. The bottom chart shows the size of the starting partial model of each lottery cycle. The inserts show the model structures at the end of cycles 210, 214, and 243, respectively.

6.4. A universal way of starting the sR1 calculation of a “difficult” case?

There is one more thing about figure 8 that is worth attention. The inserts show that at the end of cycle 210 the resulting model still had no recognizable fragments, but by the end of cycle 214 many recognizable fragments suddenly appeared. Note that cycles 211, 212 and 213 were skipped because of failing to improve the model. More shockingly, the starting partial model of cycle 214 was a single N atom at (0.8333, 0.2333, 0.1184). By some magic, this location made this sR1 cycle very successful. In comparison, the initial starting model of a single F atom at (0.3, 0.3, 0.3) was unsuccessful. This peculiar phenomenon suggests that there is subtlety on where to put the initial single atom. By the experience of applying the sR1 method to about 200 datasets, the default initial position (0.3, 0.3, 0.3) works for most cases. The observation that (0.8333, 0.2333, 0.1184) works much better than the default (0.3, 0.3, 0.3) for sample 3 indicates that, the reason that sample 3 was regarded as a “difficult” case might simply be because the default choice happened to be a bad choice for this dataset. Why does where to put the starting single atom matter? A grid of 0.4 Å step size is set up within the unit cell. The grid points are fixed within the unit cell. However, the location of the sR1 holes depends on the location of the single atom. Therefore, how well the grid points can coarsely catch the sR1 holes depends on the location of the single atom. There must be an optimal location of this single atom such that one cycle of the sR1 calculation can lead to the best tentative full model, as measured by the lowest of the minimum approximate R1. Note that each trial reaches a minimum approximate R1, and the trial with the lowest resulting minimum approximate R1 is the best trial. There is no need to search for this optimal location in the whole unit cell. Instead, a search within a small box of 0.4 Å by 0.4 Å by 0.4 Å with the corner of the lowest coordinates at (0.3, 0.3, 0.3) is sufficient. A coarse search with 4 by 4 by 4 (= 64) local grid points within this box for sample 3 yielded an optimal location of (0.325, 0.3042, 0.3). The structure of sample 3 can be successfully solved by starting lottery cycles with a partial model of a single F atom at (0.325, 0.3042, 0.3). It was observed that a dramatic drop of the approximate R1 happened at cycle 26, a cycle started with a small child model of 20 atoms. A good final model was reached at the end of cycle 85 (see more details in the supporting information). So, for a “difficult” case like the case of sample 3, a universal way to start the sR1 calculation might be to find an optimal initial location for the starting single atom. This approach seems general. It might work even when no fragments of known structure are available for running the pR1 method to jumpstart the sR1 calculation. However, this idea currently is only at the initial stage, and further tests are needed.

6.5. The effect of data resolution

The data resolution limits of samples 1 to 4 are given in Table 1. Of the four samples, 1 and 4 have higher resolutions (0.79 Å and 0.85 Å, respectively) while 2 and 3 have lower resolutions (1.0 Å and 0.90 Å, respectively). Interestingly, though sample 3 has slightly higher resolution than sample 2, 3 was regarded as a “difficult” case while 2 was not.

The effect of data resolution on the effectiveness of the sR1 method has been studied in the previous paper (Zhang & Donahue, 2024). Essentially, lower data resolution makes a structure harder to solve. When data resolution is high, a structure can be straightforwardly solved by starting from a single atom at (0.3, 0.3, 0.3). However, when data resolution is low, the case becomes more difficult. Before the lottery mode was designed, a difficult case required either intelligently guessing a correct fragment or orienting and positioning fragments of a known structure by the pR1 method to jumpstart the sR1 calculation. Now, with the lottery mode, even difficult cases can be solved by starting from a single atom (see section 6.3). Take sample 3 in the previous paper (Zhang & Donahue, 2024) as an example. Previously, when data resolution was truncated to 1 Å, different avenues had to be taken to solve the structure. For instance, one route required a fragment of 4 C atoms to be guessed. In another route, a benzene ring had to be correctly oriented through the pR1 method. Now, using the lottery mode, as shown in Figure 9, this difficult case (when data resolution is truncated to 1 Å) can be directly solved by starting from a single C atom at (0.3, 0.3, 0.3). However, the structure is solved only after 113 lottery cycles in addition to the initial sR1 cycle, in comparison, if the data resolution is 0.77 Å (Zhang & Donahue, 2024) the structure can be solved by the initial sR1 cycle only. So, clearly low data resolution makes a structure much harder to solve.

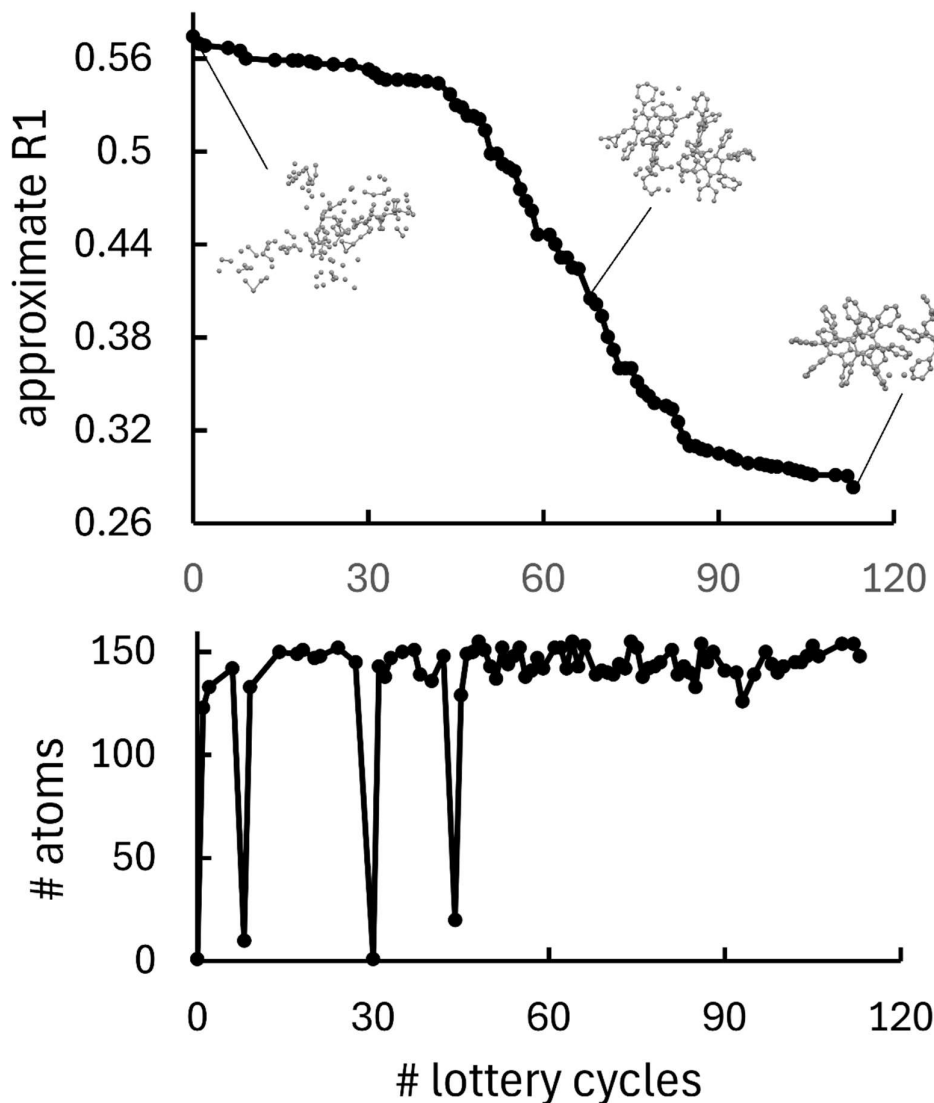


Figure 9 Solving the structure of sample 3 of a previous paper (Zhang & Donahue, 2024) when data resolution was truncated to 1 Å by running the sR1 calculation in lottery mode, starting from a single C atom at (0.3, 0.3, 0.3). The top chart shows how the minimum approximate R1 in each lottery cycle drops when the calculation proceeds. The bottom chart shows the size of the starting partial model of each lottery cycle. The inserts show the model structures at the end of cycles 0, 68, and 113, respectively.

6.6. Can a final structure “solution” be reached?

The very first word in the title of this paper is “solving”. One reviewer objected to the loose usage of “structure solution” in this paper. Therefore, it is necessary to clarify the exact claim of this paper so that a reader will not be misled.

In the above section, each resulting model was compared to a “correct” model. Here is how such a “correct” model was obtained. A structure was “solved” by the program *SHELXT* (Sheldrick, 2015a). After going through “refinement” with the program *SHELXL* (Sheldrick, 2015b) and deleting H atoms, the structure was expanded to the P1 space group. This expanded structure is the “correct” model. Therefore, the exact claim of this paper [as well as of the previous paper (Zhang & Donahue, 2024)] is that the sR1 method (with or without the assistance of the lottery mode) can “solve” a structure just as good as the program *SHELXT* can “solve” a same dataset.

A reader should bear in mind that in this paper “structure solution” only refers to a step like running the program *SHELXT*. It does not refer to a final crystallography structure solution. To clarify, the sR1 method can be used where *SHELXT* is used, except the former needs additional external help. The *Platon* program (Spek, 2020) needs to be used to determine the space group and to help to find the asymmetric unit (see an example in the supporting information). According to the reviewer, a structure can only be claimed to be solved if one of two quantitative criteria is met: either by establishing that the average phase error for all reflections (relative to published phases) is below a certain limit (say 30°-35°), or by establishing that the R is below a certain limit (say, $R < 0.16$). Because all results are started without being published, this boils down to only one criterion: a structure can only be claimed to be solved if $R < 0.16$. The author accepts this as the strict crystallography criterion of “structure solution.” According to this criterion, samples 1, 3 and 4 could reach their final solutions because their final R’s (after going through steps of determining space group and asymmetric unit and performing refinement) were 0.038, 0.075 and 0.070, respectively. However, sample 2 could not reach a final solution because its final R was 0.24. Even though a final crystallography structure solution of sample 2 could not be reached, the resulting model of this sample still revealed useful information. The author’s colleague chemists used this result as feedback that their experiments were working, because this resulting model matched their experimental expectation. However, they knew this result was unpublishable and they needed to grow a better crystal.

6.7. How well does the lottery mode work for various datasets?

The author has tested the sR1 method on about 200 datasets (see a list in the supporting information). For most cases the first sR1 cycle reveals sizable recognizable partial structure. For these cases, the lottery mode is expected to work smoothly. Indeed, a few tests have confirmed this intuition. Only when the initial sR1 cycle shows sign of trouble (namely when there are nearly no recognizable fragments) does the lottery mode have great value. In the datasets, there were a few such cases where the lottery mode necessitated use, and the results were all successful. The selected samples 1, 2 and 3 were among the most difficult ones in this group. Sample 4 was selected as a representative structure for those with many heavy atoms. Usually, structures containing many heavy atoms like sample 4 are readily solved by the sR1 method. In fact, they also fall in the group in which the first sR1 cycle

reveals sizable recognizable partial structure, therefore, no trouble was expected for these cases when applying the lottery mode. For a few datasets that could easily be solved by the sR1 method in the “intelligent” mode and could also be trivially done through the lottery mode, these datasets were still tested using the lottery mode out of curiosity. However, these cases that were subjected to the lottery mode were intentionally made more difficult. For example, instead of starting from a single atom, the model started with all atoms being randomly positioned in the unit cell. Despite the increased difficulty, the lottery mode still worked well in these tests. However, this outcome should have been “expected” because the lottery mode has been designed to have a small child model for rebuilding a model from scratch.

6.8. Conclusions

Based on the above observations, the main conclusions of this study can be summarized as follows:

(1) The designed lottery mode can drive the sR1 calculation toward correct structure solutions. (2) This new method, namely, carrying out the sR1 calculation in a lottery mode, is useful for a care-free application of the sR1 method. (3) A fast-computing tool is needed for further exploration of the sR1 method. Slow rate of calculation with Surface Pro units is limiting the author’s ability of testing various new ideas of developing the sR1 method. However, the method itself can go extremely fast if parallel programming is fully exploited and a dedicating supercomputer is accessible.

Acknowledgements Professor James P. Donahue, Professor Robert A. Pascal and Professor Joel T. Mague provided the crystal samples used in this work.

References

- Bott, R. & Sarma, R. (1976). *J. Mol. Biol.* **106**, 1037-1046.
- Bricogne, G. (1992). *Proceedings of the CCP4 Study Weekend. Molecular Replacement*, edited by W. Wolf, E. J. Dodson & S. Gover, pp. 62-75. Warrington: Daresbury Laboratory.
- Burla, M. C., Carrozzini, B., Cascarano, G. L., Giacovazzo, C. & Polidori, G. (2018). *Acta Cryst.* **A74**, 123-130.
- Burla, M. C., Carrozzini, B., Cascarano, G. L., Giacovazzo, C. & Polidori, G. (2020). *Acta Cryst.* **D76**, 9-18.
- Caliandro, R., Carrozzini, B., Cascarano, G. L., Giacovazzo, C., Mazzone, A. & Siliqi, D. (2009). *Acta Cryst.* **A65**, 512-527.
- Crowther, R. A. (1972). In *The Molecular Replacement Method*, Ed. M. G. Rossmann, Gordon & Breach, New York, pp. 173-178.

- DeTitta, G. T., Weeks, C. M., Thuman, P., Miller, R. & Hauptman, H. A. (1994). *Acta Cryst.* **A50**, 203-210.
- Emsley, P., Lohkamp, B., Scott, W. G. & Cowtan, K. (2010). *Acta Cryst.* **D66**, 486–501.
- Eventoff, W., Hackert, M. L. & Rossmann, M. G. (1975). *J. Mol. Biol.* **98**, 249-258.
- Giacovazzo, C. (2014). *Phasing in Crystallography – A Modern Perspective*. Oxford: Oxford University Press.
- Gorelik, T. E., Lukat, P., Kleeberg, C., Blankenfeldt, W. & Mueller, R. (2023). *Acta Cryst.* **A79**, 504-514.
- Kinneberg, A. J. & de Graaff, R. A. G. (1984). *J. Appl. Cryst.* **17**, 364-366.
- Lamzin, V. S., Perrakis, A. & Wilson, K. S. (2012). *International Tables for Crystallography. Vol. F, Crystallography of Biological Macromolecules*, 2nd online ed., edited by E. Arnold, D. M. Himmel and M. G. Rossmann, pp. 525–528. Dordrecht: Kluwer Academic Publishers.
- McCoy, A. J. (2004). *Acta Cryst.* **D60**, 2169-2183.
- McCoy, A. J. (2017). In *Protein Crystallography: Methods and Protocols*, Ed. A. Wlodawer, Z. Dauter & M. Jaskolski, Humana Press, New York, pp. 421-454.
- McCoy, A. J., Grosse-Kunstleve, R. W., Adams, P. D., Winn, M. D., Storoni, L. C. & Read, R. J. (2007). *J. Appl. Cryst.* **40**, 658–674.
- McCoy, A.J., Oeffner, R. D., Wrobel, A. G., Ojala, J. R., Tryggvason, K., Lohkamp, B. & Read, R. J. (2017). Ab initio solution of macromolecular crystal structures without direct methods. *Proc. Natl. Acad. Sci. USA* **114**, 3637-3641.
- Miller, R., DeTitta, G. T., Jones, R., Langs, D. A., Weeks, C. M. & Hauptman, H. A. (1993). *Science*, **259**, 1430-1433.
- Read, R. J. (2001). *Acta Cryst.* **D57**, 1373-1382.
- Read, R. J. & McCoy, A. J. (2016). *Acta Cryst.* **D72**, 375-387.
- Rossmann, M. G. (1972). Editor. *The Molecular Replacement Method*. New York: Gordon & Breach.
- Rossmann, M. G. (1990). *Acta Cryst.* **A46**, 73-82.
- Rossmann, M. G. & Blow, D. M. (1962). *Acta Cryst.* **15**, 24-31.
- Rossmann, M. G., Blow, D. M., Harding, M. M., & Collier, E. (1964). *Acta Cryst.* **17**, 338-342.
- Sheldrick, G. M. (2015a). *Acta Cryst.* **A71**, 3-8.
- Sheldrick, G. M. (2015b). *Acta Cryst.* **C71**, 3-8.
- Sheldrick, G. M. & Gould, R. O. (1995). *Acta Cryst.* **B51**, 423-431.
- Spek, A.L. (2020). *Acta Cryst.* **E76**, 1-11.
- Terwilliger, T. C., Grosse-Kunstleve, R. W., Atonine, P. V., Moriarty, N. W., Zwart, P. H., Hung, L., Read, R. J. & Adams, P. D. (2008). *Acta Cryst.* **D64**, 61-69.
- Weeks, C. M., DeTitta, G. T., Miller, R. & Hauptman, H. A. (1993). *Acta Cryst.* **D49**, 179-181.
- Zhang, X. & Donahue, J. P. (2024). *Acta Cryst.* **A80**, 237-248.

Supporting information

A note to the reader: Some information included in this supporting information is not intended to give a reader additional information. Rather, it is included for the reader's convenience to check the author's work. In this way, hidden surprise is avoided, so that a reader can be certain that the author was not making blunder mistakes.

S1. Information on data collection of the samples

All crystals were coated with paratone oil and mounted on the end of a nylon loop attached to the end of the goniometer. Data were collected at 150 K under a dry N₂ stream supplied under the control of an Oxford Cryostream 800 attachment. The data collection instrument was a Bruker D8 Quest Photon 3 diffractometer equipped with a Mo fine-focus sealed tube providing radiation at $\lambda = 0.71073$ nm or a Bruker D8 Venture diffractometer operating with a Photon 100 CMOS detector and a Cu Incoatec I microfocus source generating X-rays at $\lambda = 1.54178$ nm.

S2. Data quality is the main factor affecting an R-value

We know this by experience: often a better-quality crystal leads to better quality data and a lower R-value, even though the same set of programs (either SHELXT + SHELXL or sR1 + Platon + SHELXL) are used for data treatment.

S3. How to verify the effectiveness of the sR1 method

Though in the body of the paper a model comparison criterion has been suggested to verify that the sR1 calculation can reach approximately the same model as *SHELXT* (Sheldrick, 2015a) does when treating a same dataset, such verification is only auxiliary. In fact, there is independent way to verify the effectiveness of an sR1 result: visually inspecting the resulting model one can immediately tell if the structure has been revealed or has not been revealed at all. Such qualitative visual inspection is performed in daily work. However, it should be acknowledged that one reviewer has raised concern on the usage of such qualitative criterion:

Qualitative criterion (for example, visual recognition of molecular geometry) is not a scientific method: the molecule could be shifted compared to the real position, or could be differently oriented, or explodes when subjected to mnq. What would the user think when such case occurs?

It should be clarified that for the sR1 method this concern is unnecessary. Whole model shift is immaterial, which results in the same solution. In fact, in sR1 calculation such shift happens all the time. The sR1 method also cannot distinguish between a solution and an inverted solution. Furthermore, the sR1 method is carried out in the P1 space group. The mnq of P1 only contains an

identity operator. Upon identity operation, no “explode” is expected. Thus, the only remaining concern is a model that is incorrectly oriented. If a structure is solved by fitting a known model into an unknown structure, this concern is legitimate. However, the sR1 develops a solution in an atom-by-atom manner. A resulting model happens to be chemically recognizable but incorrectly oriented is unlikely to happen. This is because the initial partial structure guides new atoms into “correct” positions and/or atoms of “more incorrectly positioned” ones are gradually replaced by “more correctly positioned” ones. Correct relative positioning and chemical recognizability are developed together. They are two sides of the same coin. Furthermore, the method is centered on minimizing R1 value. The final model corresponds to minimum R1. This means the orientation of the resulting model is close to the best that can match the reflection data. With all these considerations, the chemical recognizability that has been developed in such a process is “the” sign that the correct model has been revealed. Therefore, for the sR1 method, qualitative visual inspection is valid evidence for verifying the effectiveness of the method.

It should be acknowledged that often an R-value is reported. The main factor affecting an R-value is the quality of the dataset (see above). Because the reliability of the resulting model does depend on the quality of the dataset, it is appropriate to report an R-value. However, an R-value alone cannot tell if a structure has been revealed or not. One still needs to visually inspect the model to be certain whether the structure has indeed been revealed or has not been revealed at all. It is obvious that no matter how low an R-value is, if no chemically recognizable model has emerged, no one would admit that the structure has been “solved”. On the other hand, if a chemically recognizable model has emerged, no matter how high the R-value is, at least the structure has been qualitatively revealed. Once it is certain that a structure has been revealed, an R-value can be cited to indicate the quality and reliability of the resulting model.

Conclusion: Visual inspection and only visual inspection can tell whether a structure has been revealed or not. Once it is certain that a structure has been revealed, an R-value can be cited to indicate the quality and reliability of the model. The purpose of the sR1 method is to reveal the structure. For this, only visual inspection can help to determine if a structure has been revealed or has not been revealed.

S4. Implementation of the Wilson method for the determination of the parameter B

The raw reflection intensities $F_o^2(hkl)$ are ranked by $s = \sin\theta/\lambda$ and are divided into either 20 groups if the total number of reflections exceeds 10000 or 10 groups otherwise. For each group, calculate the average intensity which is denoted as $\langle F_o^2 \rangle$, and the average s value which is denoted as $\langle s \rangle$. This leads to the following approximate equation:

$$k \langle F_o^2 \rangle \approx \left[\sum_j f_j^2 (\langle s \rangle) \right] \exp(-2B \langle s \rangle^2)$$

In this equation, k is a scaling constant for the observed intensities, and B is the parameter whose value is sought for.

This equation can convert into a linear form of $Y = a + bX$, in which X and Y are defined as:

$$X = \langle s \rangle^2$$

$$Y = \ln \frac{\langle F_o^2 \rangle}{\sum_j f_j^2 (\langle s \rangle)}$$

and the intercept a and the slope b are:

$$a = -\ln(k)$$

$$b = -2B$$

After calculating the (X, Y) data points for all the groups use linear fit to find the intercept a and the slope b , and further calculate the parameters k and B as follows:

$$k = \exp(-a)$$

$$B = -b/2$$

Once the parameter B is obtained, a sharpened intensity is calculated as:

$$(F_o^2)_{sharpened} = F_o^2 \exp(2Bs^2)$$

However, the sharpened intensities are not scaled by multiplying with the scaling constant k ; instead, they are scaled such that their sum equals $\sum_{hkl} \sum_j f_j^2(hkl)$.

S5. The algorithm of comparing two models

This algorithm only compares the positions of the atoms in the two models; it disregards the types of atoms. Let a , b , and c be the length of the unit cell edges. One difficulty of making this comparison is that the two models may have different locations relative to the unit cell edges. The algorithm uses an approximate method to overcome this difficulty: shift all atoms of one model (model A) such that one of its atoms overlaps one atom of the other model (model B). Try this for all atoms in both models. So, the calculation needs to be repeated for $N_A \times N_B$ times, where N_A and N_B are the number of atoms in the models A and B, respectively. Further these calculations also need to be repeated after inverting model B, in case model A matches the inverted version of B better. After repeating the calculation, use the result of the best match that has been discovered.

After overlapping one atom of model A with a particular atom of model B by properly shifting all atoms of model A, we make sure all atoms of both models are located within the unit cell (by adding 1 to or subtracting 1 from the fractional coordinates x, y, z of an atom). With such preparation we are ready to count how many atoms of A are each within $s = 0.5 \text{ \AA}$ of an atom in B. To make such

comparison quick, we convert the fractional coordinates x, y, z of an atom to integers in the following way:

$$N_x = \text{int}(a/s), N_y = \text{int}(b/s), N_z = \text{int}(c/s)$$

$$I_x = \text{int}(xN_x), I_y = \text{int}(yN_y), I_z = \text{int}(zN_z)$$

Thus, (I_x, I_y, I_z) is the integer coordinate of an atom.

Prepare a mask $M_A(i, j, k)$ for model A, where $i = 0$ to $N_x - 1$, $j = 0$ to $N_y - 1$, and $k = 0$ to $N_z - 1$. $M_A(i, j, k)$ takes value 0 unless (i, j, k) is the integer coordinate of an atom. In that case, it takes value 1. Similarly, $M_B(i, j, k)$ is a mask for model B.

The number of atoms of model A which overlap within 0.5 \AA with an atom of B can be calculated as $\sum_{i,j,k} M_A(i, j, k)M_B(i, j, k)$.

S6. Technical details of using pR1 to determine the orientation of a fragment as well as to position a fragment of a known orientation

A local Cartesian coordinate system is set up for the fragment by selecting a local origin and three orthogonal directions.

A Cartesian coordinate system is also set up for the unit cell. The origin of this system overlaps the origin of the unit cell. Its three unit vectors \mathbf{x} , \mathbf{y} , and \mathbf{z} are related to the cell vectors \mathbf{a} and \mathbf{b} as follows: $\mathbf{x} = \mathbf{a}/|\mathbf{a}|$, $\mathbf{y} = (\mathbf{b} - \mathbf{b} \cdot \mathbf{x})/|\mathbf{b} - \mathbf{b} \cdot \mathbf{x}|$, $\mathbf{z} = \mathbf{x} \times \mathbf{y}$. The Cartesian coordinates and the fractional coordinates of an atom in the unit cell are inter-converted during the calculations. Using cell parameters a, b, c, α, β , and γ , the relation between fractional coordinates (x_f, y_f, z_f) and Cartesian coordinates (x_c, y_c, z_c) is expressed as:

$$\begin{pmatrix} x_c \\ y_c \\ z_c \end{pmatrix} = \begin{pmatrix} a & b \cos \gamma & c \cos \beta \\ 0 & b \sin \gamma & \frac{c(\cos \alpha - \cos \beta \cos \gamma)}{\sin \gamma} \\ 0 & 0 & \frac{V}{ab \sin \gamma} \end{pmatrix} \begin{pmatrix} x_f \\ y_f \\ z_f \end{pmatrix}$$

in which the cell volume V is calculated as:

$$V = abc \sqrt{1 - \cos^2 \alpha - \cos^2 \beta - \cos^2 \gamma + 2 \cos \alpha \times \cos \beta \times \cos \gamma}$$

At start, a fragment is positioned such that its local Cartesian system overlaps the Cartesian system of the unit cell. The fragment is attached to its local Cartesian system. So, rotation and translation of the fragment is realized by rotating and translating its local Cartesian system in the cell Cartesian system. Translation is realized by translating the local origin in the cell Cartesian system (or rather in the cell fractional coordinate system, and the fractional coordinates and the cell Cartesian coordinates are inter-converted). A general rotation is consisted by three simple rotations: a rotation around x-axis (of

the local frame) in the direction from y-axis to z-axis through angle ψ ; a rotation around z-axis (of the local frame) in the direction from x-axis to y-axis through angle φ ; and another rotation around x-axis (of the local frame) in the direction from y-axis to z-axis through angle ζ . Before rotation, a point has Cartesian coordinates (x,y,z) . After a rotation of angles (ψ,φ,ζ) , the point moves to a new location in the same Cartesian system with Cartesian coordinates (x',y',z') , which are calculated by:

$$\begin{pmatrix} x' \\ y' \\ z' \end{pmatrix} = \begin{pmatrix} 1 & 0 & 0 \\ 0 & \cos\psi & -\sin\psi \\ 0 & \sin\psi & \cos\psi \end{pmatrix} \begin{pmatrix} \cos\varphi & -\sin\varphi & 0 \\ \sin\varphi & \cos\varphi & 0 \\ 0 & 0 & 1 \end{pmatrix} \begin{pmatrix} 1 & 0 & 0 \\ 0 & \cos\zeta & -\sin\zeta \\ 0 & \sin\zeta & \cos\zeta \end{pmatrix} \begin{pmatrix} x \\ y \\ z \end{pmatrix}$$

In general, to cover all possible rotations, the range of ψ should be 0 to 360 degrees, the range of φ should be 0 to 180 degrees, and the range of ζ should be 0 to 360 degrees. When a fragment has n-fold rotation symmetry and the rotation axis is along the x-axis of its local Cartesian system, then the range of ζ can reduce to 0 to 360/n degrees.

The space spanned by rotation and translation is a 6-dimensional orientation-location space. (It is 5-dimensional if the fragment is linear.) To coarsely locate the global minimum point or the local minimum points (the holes) of a pR1 map in this 6-dimensional space, a grid is set up with 0.4 Å step size in translations within the cell and 5-degree step size in rotation angles. The range of the rotation angles are: 0 to 360 degrees for ψ , 0 to 180 degrees for φ , and 0 to 360 degrees for ζ . If the fragment has n-fold rotation symmetry, and the rotation axis is arranged along the local x-axis, the range of ζ can reduce to 0 to 360/n. The precision of locating the global minimum point or the local minimum points is refined by halving the step size locally five times.

The general hypothesis is that the deepest hole of a pR1 map in a 6-dimensional orientation-location space determines the orientation and location of a missing fragment (Zhang & Donahue, 2024). Note that by “location of a fragment” we mean the location of the local origin of the fragment (while keeping its orientation unchanged); similarly, “locating a fragment” means locating the local origin of a fragment. Determining pR1 holes in a 6-dimensional space is time-consuming. To cut calculation time, the problem is divided into two 3-dimensional calculations, that is, finding the orientation and the location in two separate steps.

For a free-standing fragment, that is, a model consisting of a single fragment with no other known atoms, the pR1 only depends on the orientation of the fragment. Therefore, the possible orientations of all missing fragments are detected by the holes in this pR1 map of a free-standing fragment in a 3-dimensional orientation space. Due to the possible symmetry of a fragment and the redundancy in representing an orientation with the three rotation angles, many orientation representations are equivalent to each other. Considering two orientation representations, if the atoms of the fragment of one orientation representation can match the atoms of the fragment of the other representation in a one-to-one basis within 0.25 Å (see the algorithm for this type of comparison in section S3), the two

representations are considered equivalent. The non-equivalent orientation representations are filtered out from all detected representations. These serve as the candidate orientations.

The candidate orientations are ranked from the smallest R1 to the highest R1 and are labelled by 0, 1, 2, etc. In some situations, for example, if it is known that there are only two fragments in the structure, then it is obvious that one fragment has orientation 0 and the other has orientation 1. In such a situation, fragment 0 takes orientation 0, and its location is determined by the deepest hole in a pR1 map of a 3-dimensional location space. After determination of fragment 0, a new pR1 is defined by including the atoms of fragment 0 as known atoms and taking orientation 1 the location of fragment 1 is determined by the deepest hole of this new pR1 map in a 3-dimensional location space. In other situations, there are multiple fragments in the structure. In such situations, to determine a missing fragment, it is necessary to try all possible orientations. For each trial orientation, the best choice of location of a missing fragment is determined by the deepest hole in a pR1 map of a 3-dimensional location space. This best choice is combined with the trial orientation to form a candidate orientation-location. Trying all candidate orientations leads to a list of candidates of orientation-locations which can be ranked from the smallest R1 to the highest R1. The missing fragment is determined by the candidate orientation-location of the lowest R1. With this missing fragment being determined, a newer pR1 is defined by including the atoms of the newly determined fragment as known atoms. This newer pR1 is used to determine the next missing fragment in the same way.

When using the single atom R1 (sR1) to locate single missing atoms (Zhang & Donahue, 2024), a rule excluding clustering ghost atoms and a rule excluding triangular bonding are enforced. Similarly, here, when using pR1 to locate a missing fragment, these rules are also enforced: if a trial orientation-location for a missing fragment will cause one of its atoms being a clustering ghost atom, or one of its atoms will involve triangular bonding with two known atoms, this trial is disqualified as a candidate for determining the orientation-location of the missing fragment.

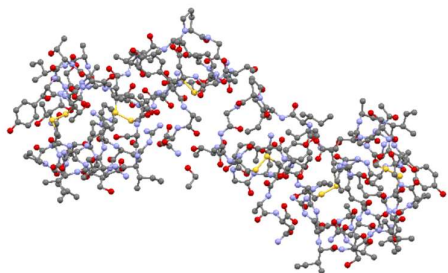
S7. An attempt of solving a protein structure by the sR1 method

The data of this SI form crambin (a plant seed protein) is taken from the Protein Data Bank (code: 1AB1; Yamao, Heo & Teeter, 1997). Here is its crystallographic information:

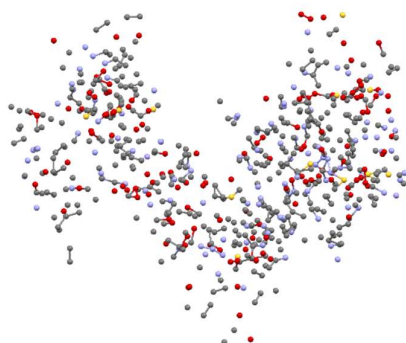
Sample	Formula (excluding H)	Z	non- hydrogen atoms in cell	a(Å)	b(Å)	c(Å)	$\alpha(^{\circ})$	$\beta(^{\circ})$	$\gamma(^{\circ})$	space group
crambin	$S_6O_{66}N_{55}C_{202}$	2	658	40.76	18.40	22.27	90.00	90.70	90.00	P2 ₁

There are 658 non-hydrogen atoms in its unit cell, including 12 S atoms.

The correct model of this protein is:



Running one cycle of the sR1 method by starting with a single S atom at (0.3, 0.3, 0.3) yields a model with no recognizable fragments:

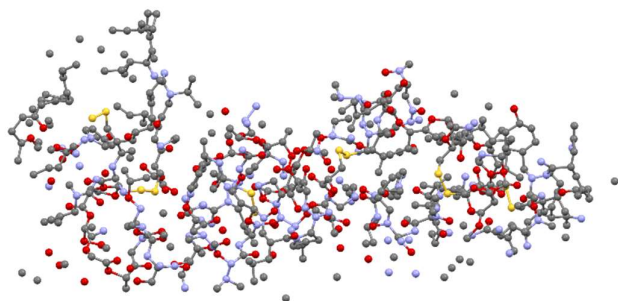


The structure contains six benzene rings, but the pR1 method cannot locate these rings, probably because the 12 S atoms have not been located yet.

To test if the sR1 method has any power on this structure, an sR1 calculation has been performed by starting with a partial structure of the 12 S atoms at their correct positions:



The calculation proceeds in mix of lottery mode and intelligent mode, and the following model is reached:



Compared with the correct model, this result has 588 atoms located within 0.5 Å of their corresponding correct locations, with only 70 atoms being misplaced. So, this is a very encouraging result. And it is expected that this result can be greatly improved after deleting the “ghost” atoms and discovering the missing atoms by the bond length guided sR1 method.

Further study should focus on how to jumpstart the sR1 calculation. But a fast-computing tool is needed, because currently running on a Surface Pro 9 unit (the author owns both Surface Pro 7 and 9), one sR1 cycle needs about 3 hours. With such a slow pace, it is hard to test various ideas of jumpstarting the calculation.

S8. A universal way of starting the sR1 calculation of a “difficult” case?

There is one more thing about figure 8 that is worth attention. The inserts of figure 8 show that at the end of cycle 210 the resulting model still had no recognizable fragments, but by the end of cycle 214 many recognizable fragments suddenly appeared. Note that cycles 211, 212 and 213 were skipped because of failing to improve the model. More shockingly, the starting partial model of cycle 214 was a single N atom at (0.8333, 0.2333, 0.1184). By some magic, this location made this sR1 cycle very successful. In comparison, the initial starting model of a single F atom at (0.3, 0.3, 0.3) was unsuccessful. This peculiar phenomenon suggests that there is subtlety on where to put the initial single atom. By the experience of applying the sR1 method to about 200 datasets, the default initial position (0.3, 0.3, 0.3) works for most cases. The observation that (0.8333, 0.2333, 0.1184) works much better than the default (0.3, 0.3, 0.3) for sample 3 indicates that, the reason that sample 3 was regarded as a “difficult” case might simply was because the default choice happened to be a bad choice for this dataset. Why does where to put the starting single atom matter? A grid of 0.4 Å step size is set up within the unit cell. The grid points are fixed within the unit cell. However, the location of the sR1 holes depends on the location of the single atom. Therefore, how well the grid points can coarsely catch the sR1 holes depends on the location of the single atom. There must be an optimal location of this single atom such that one cycle of the sR1 calculation can lead to the best tentative full model, as measured by the lowest of the minimum approximate R1. Note that each trial reaches a minimum approximate R1, and the trial with the lowest resulting minimum approximate R1 is the best trial. There is no need to search for this optimal location in the whole unit cell. Instead, a search within a small box of 0.4 Å by 0.4 Å by 0.4 Å with the corner of the lowest coordinates at (0.3, 0.3, 0.3) is sufficient. A coarse search with 4 by 4 by 4 (= 64) local grid points within this box for sample 3 yielded an optimal location of (0.325, 0.3042, 0.3). The structure of sample 3 can be successfully solved by starting lottery cycles with a partial model of a single F atom at (0.325, 0.3042, 0.3):

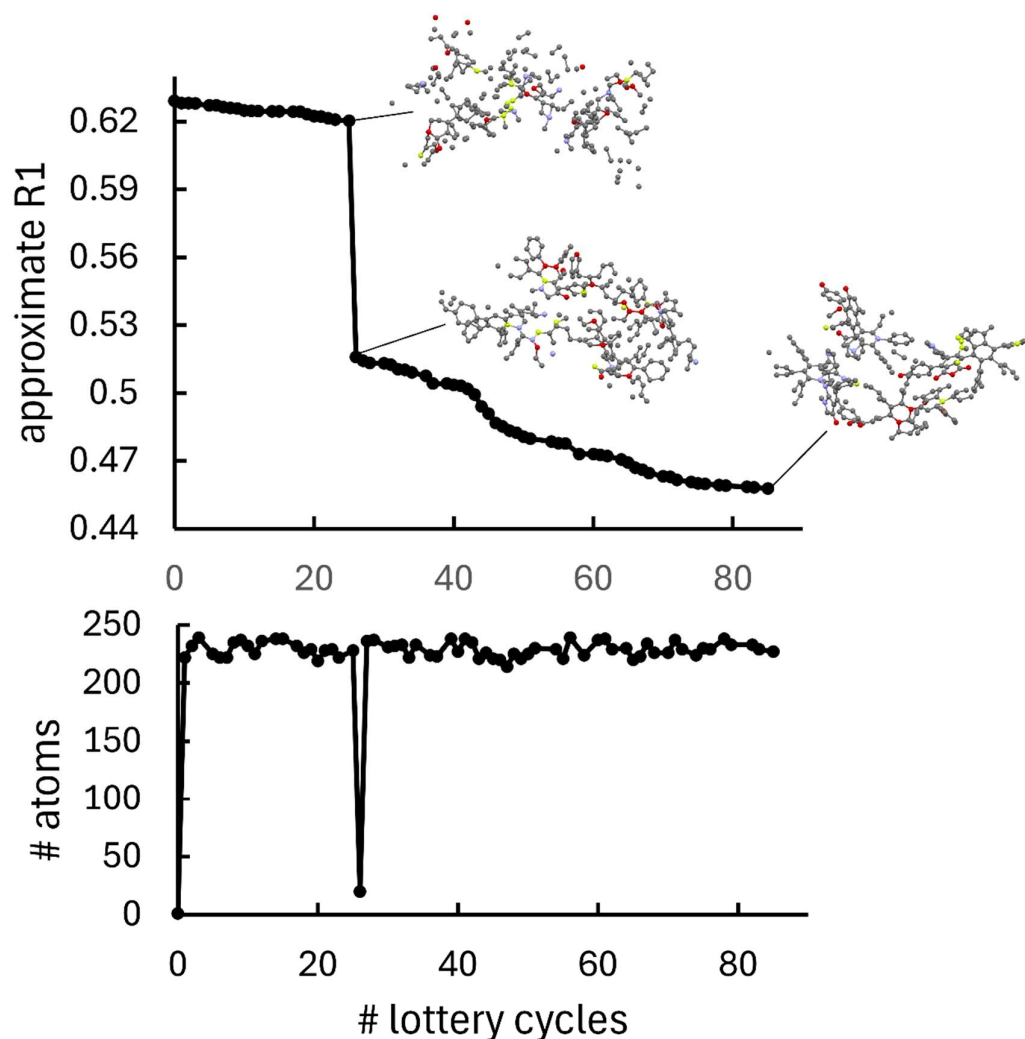


Figure S1 Solving the structure of sample 3 by running the sR1 calculation in the lottery mode, starting from a single F atom at (0.325, 0.3042, 0.3). The top chart shows how the minimum approximate R1 that has been reached in each lottery cycle drops when the calculation proceeds. The bottom chart shows the size of the starting partial model of each lottery cycle. The inserts show the model structures at the end of cycles 25, 26, and 85, respectively.

It was observed that a dramatic drop of the approximate R1 happened at cycle 26, a cycle started with a small child model of 20 atoms. A good final model was reached at the end of cycle 85. So, for a “difficult” case like the case of sample 3, a proper way to start the sR1 calculation is to find an optimal initial location for the starting single atom. This approach is general. It works even when no fragments of known structure are available for running the pR1 method to jumpstart the sR1 calculation. However, more study needs to be done on the effectiveness of this method.

Exact mathematical details are given in this paragraph: Let a , b , and c be the size of the unit cell, and $s = 0.4 \text{ \AA}$ be the step size of the grid. Calculate integers $N_x = \text{int}(a/s)$, $N_y = \text{int}(b/s)$, and $N_z =$

$int(c/s)$. The grid points inside the cell are set at $x = i/N_x$, $y = j/N_y$, and $z = k/N_z$ for i from 0 to $N_x - 1$, j from 0 to $N_y - 1$, and k from 0 to $N_z - 1$. Let $N_{cut} = 4$. Local grid points are set nearby point (0.3, 0.3, 0.3) at $x = 0.3 + i/N_x/N_{cut}$, $y = 0.3 + j/N_y/N_{cut}$, and $z = 0.3 + k/N_z/N_{cut}$ for i from 0 to $N_{cut} - 1$, j from 0 to $N_{cut} - 1$, and k from 0 to $N_{cut} - 1$. There are total $N_{cut}^3 = 64$ local grid points. Perform one cycle of sR1 calculation by starting from a single F atom at each local grid point to find which local grid point can lead to an optimal tentative full model.

S9. Using the Platon program to determine the space group and extracting the asymmetric unit

The sR1 method solves a structure in the minimal P1 space group. To find the correct space group, the result is checked by the *Platon* program (Spek, 2020). Using sample 3 as an example, the procedure is explained here. Checking the sR1 result of sample 3 the *Platon* gives following result:

```
Space Group H-M: P21/c                               Laue: 2/m
Space Group Hall: -P 2ybc                             [Schoenflies: C2h^5 ]
Lattice Type: mP, Centric, Monoclinic, Multiplicity: 4( 2), No: 14
```

Non-Sohnke - No Absolute Structure

```
Nr          ***** Symmetry Operation(s) *****
```

```
1           X ,           Y ,           Z
2           - X ,          1/2 + Y ,          1/2 - Z
3           - X ,           - Y ,           - Z
4           X ,           1/2 - Y ,          1/2 + Z
```

```
:: Origin Shifted to: 0.0985,-0.2459, 0.0497 after Transformation
```

```
::                               ( 0.0000  0.0000  1.0000) ( -0.0985)
:: R/t for Coordinates           ( 0.0000 -1.0000  0.0000) (  0.2459)
::                               ( 1.0000  0.0000  0.0000) ( -0.0497)
```

So, the space group is P2₁/c. *Platon* also suggests how the coordinates should be transformed, including shift of origin to match the convention. Namely, new coordinates (x, y, z) are related to the old coordinates (x', y', z') by $x = z' - 0.0985$, $y = -y' + 0.2459$, and $z = x' - 0.0497$. Similarly, new hkl are related to the old h'k'l' by $h = l'$, $k = -k'$, and $l = h'$. Convert xyz and hkl according to these rules. Also switch cell parameter a with c. Because there are four symmetry operators and four molecules in

judgment was used. Of course, some datasets simply have no solution. However, only those datasets that can be solved by the *SHELXT* program are selected to test with sR1 method, so, all the selected datasets are solvable.

The following table lists datasets that have been tested by the sR1 method. Note that hydrogen atoms are omitted in the cell content and in the asymmetric unit. There are 224 datasets, among which 64 are light atoms only. Note that some datasets repeat the same compound when multiple datasets are acquired in a process of searching for a better quality. Some compounds also have crystals of different unit cells. The structures of these 224 datasets have been solved by the sR1 method, resulting in recognizable models. Most datasets are solved straightforwardly by starting from a single atom at (0.3, 0.3, 0.3). But there are 3 datasets (those labeled with letter “D”) appear to be difficult and require using the pR1 method to put some fragment(s) of a known structure to jumpstart the sR1 calculation. 21 datasets (those labeled with letter “L”) have been tested with the lottery mode. For most datasets there is no need to test with the lottery mode, because the very first sR1 cycle already reveals a sizable recognizable partial structure, therefore, it is expected that the lottery mode will work trivially. Note that no new information is gained from the additional lottery mode tests, because the selected four examples in the body of the paper have well represented these tests.

Sample	Cell content	Asymmetric unit	a(Å)	b(Å)	c(Å)	$\alpha(^{\circ})$	$\beta(^{\circ})$	$\gamma(^{\circ})$	space group
1L	(FN ₂ C ₁₃) ₈	FN ₂ C ₁₃	8.45	9.93	24.20	90.00	90.00	90.00	Pbca
2L	(O ₂ C ₂₉) ₈	O ₂ C ₂₉	44.17	10.73	8.93	90.00	90.00	90.00	Pbcn
3L	(F ₂ O ₄ N ₂ C ₅₂) ₄	F ₂ O ₄ N ₂ C ₅₂	12.27	24.23	15.42	90.00	96.94	90.00	P2 ₁ /c
4LD	(PdS ₆ P ₄ C ₆₈) ₄	PdS ₆ P ₄ C ₆₈	23.32	14.45	22.39	90.00	115.22	90.00	P2 ₁ /c
5L	(S ₂ O ₂ C ₁₂) ₂	S ₂ O ₂ C ₁₂	5.86	10.34	10.74	90.00	104.50	90.00	P2 ₁
6L	C ₄₆	C ₂₃	5.95	10.80	12.97	103.77	99.95	90.46	P-1
7L	(C ₇₈) ₂	C ₇₈	12.34	15.98	16.57	114.10	90.70	103.20	P-1
8L	(ION ₂ C ₇) ₄	ION ₂ C ₇	18.34	7.18	8.26	90.00	90.00	90.00	Pnma
9	(PtP ₂ S ₄ N ₄ O ₃ C ₄₃) ₂	PtP ₂ S ₄ N ₄ O ₃ C ₄₃	11.60	14.16	14.99	68.04	68.02	74.14	P-1
10	(MoSiO ₄ NC ₂₈) ₈	MoSiO ₄ NC ₂₈	36.36	10.22	20.00	90.00	111.34	90.00	C2/c
11	(IMo ₃ S ₁₃ N ₃ C ₂₇) ₄	IMo ₃ S ₁₃ N ₃ C ₂₇	12.97	37.99	11.64	90.00	91.72	90.00	P2 ₁ /c
12	(INC ₈) ₈	INC ₈	23.13	8.34	14.88	90.00	126.57	90.00	C2/c
13	(MoC ₂₁) ₆	Mo _{1/3} C ₇	12.59	12.59	19.54	90.00	90.00	120.00	R-3
14	(NiS ₂ N ₂ C ₁₈) ₄	NiS ₂ N ₂ C ₁₈	11.45	10.91	16.37	90.00	104.16	90.00	P2 ₁ /n
15	Pd ₂ Cl ₄ P ₄ O ₂ N ₄ C ₂₈	PdCl ₂ P ₂ ON ₂ C ₁₄	7.28	10.62	12.94	75.02	80.91	88.73	P-1
16L	(NiS ₂ N ₂ C ₁₈) ₄	NiS ₂ N ₂ C ₁₈	11.43	10.93	16.40	90.00	104.16	90.00	P2 ₁ /n
17L	(S ₈) ₁₆	S ₄	10.38	12.75	24.43	90.00	90.00	90.00	Fddd
18	(PtCl ₄ S ₄ C ₂₀) ₁₆	(PtCl ₄ S ₄ C ₂₀) ₂	24.48	18.82	29.59	90.00	101.18	90.00	C2/c
19	S ₄ P ₂ O ₄ C ₁₂	S ₂ PO ₂ C ₆	8.10	8.35	8.47	97.73	111.08	94.68	P-1
20L	(Cl ₄ O ₂ C ₁₄) ₂	Cl ₂ OC ₇	12.24	14.04	3.83	90.00	90.00	90.00	Pba2
21L	(NiCl ₈ S ₄ C ₂₈) ₄	NiCl ₈ S ₄ C ₂₈	8.25	15.58	23.86	90.00	90.00	94.69	P2 ₁ /c
22	(RePtBrS ₂ P ₄ O ₄ C ₈₂) ₄	(RePtBrS ₂ P ₄ O ₄ C ₈₂) ₂	12.59	23.36	25.24	105.83	103.93	96.80	P-1
23	(IMo ₆ S ₂₆ P ₆ O ₁₂ C ₃₆) ₄	(IMo ₆ S ₂₆ P ₆ O ₁₂ C ₃₆) ₂	14.91	25.33	29.11	115.70	94.87	94.08	P-1
24	(CuP ₃ F ₆ N ₂ C ₅₂) ₄	CuP ₃ F ₆ N ₂ C ₅₂	11.11	23.80	17.53	90.00	100.48	90.00	P2 ₁ /n
25	Mo ₈ Si ₄ O ₃₄ C ₆₀	Mo ₄ Si ₂ O ₁₇ C ₃₀	13.82	14.01	14.16	70.76	73.31	89.62	P-1
26	(AgCl ₂ Si ₂ OC ₃₆) ₈	AgCl ₂ Si ₂ OC ₃₆	19.56	15.89	20.14	90.00	90.00	90.00	Pbca
27L	S ₆ C ₂₄	S ₃ C ₁₂	9.14	9.61	9.90	72.06	71.95	63.88	P-1
28	(PtS ₆ P ₄ C ₇₆) ₈	(PtS ₆ P ₄ C ₇₆) ₄	15.14	29.38	30.52	90.00	88.76	90.00	P-1
29	(IMo ₃ S ₁₃ N ₃ C ₂₇) ₄	(IMo ₃ S ₁₃ N ₃ C ₂₇) ₂	11.87	37.77	13.14	90.00	92.34	90.00	P-1
30	(AgCl ₂ Si ₂ OC ₃₆) ₈	AgCl ₂ Si ₂ OC ₃₆	19.55	15.89	20.15	90.00	90.00	90.00	Pbca
31	(IMo ₃ Se ₇ S ₆ P ₃ O ₆ C ₁₈) ₈	(IMo ₃ Se ₇ S ₆ P ₃ O ₆ C ₁₈) ₂	27.85	10.90	35.66	90.00	109.78	90.00	P2 ₁ /n
32	(IP ₃ OC ₅₂) ₂	IP ₃ OC ₅₂	9.80	18.49	12.97	90.00	103.33	90.00	P2 ₁
33	(IP ₃ OC ₅₂) ₂	IP ₃ OC ₅₂	9.81	18.51	12.97	90.00	103.33	90.00	P2 ₁
34	(Mo ₂ Se ₆ O ₂ N ₂ C ₁₈) ₄	Mo ₂ Se ₆ O ₂ N ₂ C ₁₈	11.33	17.93	14.56	90.00	95.77	90.00	Cc
35	Mo ₆ S ₈ P ₆ C ₁₂	Mo ₃ S ₄ P ₃ C ₆	11.84	11.98	12.07	101.76	115.33	97.00	P-1
36	(Mo ₃ Se ₇ S ₈ P ₄ O ₈ C ₂₄) ₂	Mo ₃ Se ₇ S ₈ P ₄ O ₈ C ₂₄	13.76	14.36	16.19	72.26	72.91	68.91	P-1
37	(Pd ₂ S ₁₂ C ₁₁₄) ₄	(Pd ₂ S ₁₂ C ₁₁₄) ₂	16.59	22.59	23.34	76.14	70.26	69.77	P-1
38	(Mo ₃ Si ₂ O ₁₁ C ₃₆) ₂	Mo ₃ Si ₂ O ₁₁ C ₃₆	11.31	13.41	13.49	61.45	84.55	87.81	P-1
39	(MoS ₃ Si ₂ O ₂ C ₃₆) ₄	(MoS ₃ Si ₂ O ₂ C ₃₆) ₂	11.12	13.24	23.89	90.00	96.73	90.00	P2 ₁
40L	(Cl ₂ O ₂ C ₁₄) ₄	Cl ₂ O ₂ C ₁₄	17.76	3.86	17.99	90.00	102.76	90.00	P2/n
41L	(NiCl ₈ S ₄ C ₂₈) ₄	NiCl ₈ S ₄ C ₂₈	15.69	24.07	8.34	90.00	94.80	90.00	P2 ₁ /c
42L	(NiCl ₂ S ₂ P ₂ C ₄₄) ₂	NiCl ₂ S ₂ P ₂ C ₄₄	12.11	12.11	14.63	67.01	79.65	73.17	P-1
43	(Cl ₄ O ₂ C ₁₄) ₄	Cl ₄ O ₂ C ₁₄	18.59	3.82	18.59	90.00	97.96	90.00	P2/m
44L	(Cl ₄ O ₂ C ₁₄) ₂	Cl ₂ OC ₇	12.18	14.04	3.83	90.00	90.00	90.00	Pba2

Sample	Cell content	Asymmetric unit	a(Å)	b(Å)	c(Å)	$\alpha(^{\circ})$	$\beta(^{\circ})$	$\gamma(^{\circ})$	space group
45	(SO ₃ NC ₁₃) ₂	(SO ₃ NC ₁₃) ₂	7.44	7.42	10.60	89.98	75.82	89.98	P1
46	(SN ₂ C ₁₆) ₂	SN ₂ C ₁₆	6.96	9.00	12.25	92.74	95.60	106.98	P-1
47	(SO ₂ N ₂ C ₂₆) ₄	(SO ₂ N ₂ C ₂₆) ₂	12.17	13.18	14.58	91.76	107.65	98.31	P-1
48	(CuS ₂ P ₂ F ₁₂ N ₈ C ₁₈) ₂	Cu _{1/2} SPF ₆ N ₄ C ₉	10.93	14.67	8.14	90.00	90.00	90.00	P2 ₁ 2 ₁ 2
49	(C ₃₂) ₄	C ₃₂	11.27	14.80	15.78	90.00	97.94	90.00	P2 ₁ /n
50	(W ₂ S ₈ N ₂ C ₁₈) ₄	W ₂ S ₈ N ₂ C ₁₈	19.90	9.74	16.68	90.00	112.11	90.00	P2 ₁ /c
51	(C ₁₉ ON ₂) ₄	C ₁₉ ON ₂	10.84	17.82	9.55	90.00	94.39	90.00	P2 ₁ /c
52	(C ₃₆ S ₂) ₂	C ₁₈ S	6.30	15.58	14.80	90.00	102.11	90.00	P2 ₁ /c
53	(C ₃₀ F ₂) ₂	C ₁₅ F	5.82	11.97	15.17	90.00	94.03	90.00	P2 ₁ /c
54	(W ₃ IS ₁₃ N ₃ C ₃₇) ₄	W ₃ IS ₁₃ N ₃ C ₃₇	12.97	38.01	11.75	90.00	91.46	90.00	P2 ₁ /c
55	(PtCl ₄ P ₂ C ₂₈) ₈	(PtCl ₄ P ₂ C ₂₈) ₂	18.09	18.34	16.41	90.00	90.00	90.00	P2 ₁ /c
56	(F ₄ C ₁₈) ₄	F ₂ C ₉	5.77	28.74	7.62	90.00	90.00	90.00	C222 ₁
57	(Ni ₆ S ₁₂ C ₈₄) ₈	Ni ₆ S ₁₂ C ₈₄	26.05	26.23	26.38	90.00	90.00	90.00	Pbca
58	(Ni ₆ S ₁₂ C ₈₄) ₈	Ni ₆ S ₁₂ C ₈₄	25.99	26.18	26.35	90.00	90.00	90.00	Pbca
59	(KCl ₂ O ₁₂ N ₄ C ₁₂) ₃	(KCl ₂ O ₁₂ N ₄ C ₁₂) ₃	10.81	10.83	11.92	82.07	85.23	67.92	P1
60	(KS ₂ P ₂ O ₇ NC ₁₄) ₄	KS ₂ P ₂ O ₇ NC ₁₄	11.72	17.50	13.06	90.00	114.12	90.00	P2 ₁ /c
61	(KClO ₅ N ₂ C ₆) ₆	(KClO ₅ N ₂ C ₆) ₃	10.87	10.89	11.94	82.20	85.03	67.60	P-1
62	(PtPdCl ₅ S ₆ P ₄ C ₁₀₅) ₄	(PtPdCl ₅ S ₆ P ₄ C ₁₀₅) ₂	16.47	23.10	31.39	71.40	90.00	90.00	P-1
63	(W ₃ BrS ₁₃ N ₃ C ₃₃) ₄	W ₃ BrS ₁₃ N ₃ C ₃₃	13.23	37.62	11.71	90.00	93.21	90.00	P2 ₁ /c
64L	(NiCl ₄ S ₂ P ₂ C ₄₅) ₄	NiCl ₄ S ₂ P ₂ C ₄₅	13.90	19.39	15.06	90.00	93.68	90.00	P2 ₁ /c
65	(NiS ₂ P ₂ O ₆ C ₄₅) ₄	(NiS ₂ P ₂ O ₆ C ₄₅) ₂	17.85	18.15	18.79	110.13	109.75	92.46	P-1
66L	(S ₄ C ₃₀) ₄	S ₄ C ₃₀	11.86	20.68	11.77	90.00	90.50	90.00	P2 ₁ /c
67	(P ₂ O ₆ NC ₄) ₄	P ₂ O ₆ NC ₄	7.95	10.19	11.75	90.00	91.79	90.00	Cc
68	(PtPdCl ₈ S ₆ P ₄ C ₁₀₄) ₄	PtPdCl ₈ S ₆ P ₄ C ₁₀₄	22.85	17.13	31.68	90.00	107.09	90.00	P2 ₁ /c
69	(Ni ₆ CoS ₁₂ NC ₁₀₆) ₈	Ni ₆ CoS ₁₂ NC ₁₀₆	25.95	18.38	43.06	90.00	94.06	90.00	C2/c
70	(Mo ₃ S ₁₂ ON ₅ C ₂₇) ₄	Mo ₃ S ₁₂ ON ₅ C ₂₇	21.87	10.34	19.77	90.00	94.80	90.00	P2 ₁ /c
71	(SP ₄ O ₁₂ C ₂₇) ₂	SP ₄ O ₁₂ C ₂₇	12.21	12.22	17.30	104.50	96.39	118.79	P-1
72	(IMo ₃ Se ₇ S ₆ N ₃ C ₂₇) ₁₂	(IMo ₃ Se ₇ S ₆ N ₃ C ₂₇) ₃	27.76	13.57	40.82	90.00	91.02	90.00	P2 ₁ /c
73	(IMo ₃ Se ₃ S ₁₀ N ₃ C ₂₇) ₁₂	(IMo ₃ Se ₃ S ₁₀ N ₃ C ₂₇) ₃	27.75	13.64	46.36	90.00	101.69	90.00	P2 ₁ /n
74	(IN ₃ C ₅) ₄	(IN ₃ C ₅) ₂	10.05	10.04	10.96	117.07	117.04	90.42	P-1
75	(ClSiO ₃ C ₁₇) ₈	(ClSiO ₃ C ₁₇) ₂	17.41	9.48	22.74	90.00	92.53	90.00	P2 ₁ /n
76	(O ₂ N ₅ C ₂₅) ₄	O ₂ N ₅ C ₂₅	18.61	4.98	22.69	90.00	99.48	90.00	P2 ₁ /n
77	(ClSO ₄ NC ₁₆) ₈	ClSO ₄ NC ₁₆	9.57	15.01	21.98	90.00	90.00	90.00	Pbca
78	(O ₂ N ₃ C ₂₅) ₄	O ₂ N ₃ C ₂₅	17.49	7.09	17.65	90.00	105.77	90.00	P2 ₁ /c
79	(BrO ₂ N ₄ C ₃₃) ₄	BrO ₂ N ₄ C ₃₃	13.12	14.54	15.56	90.00	107.12	9.00	P2 ₁ /n
80	(O ₆ C ₁₃) ₈	(O ₆ C ₁₃) ₂	7.12	9.64	39.66	90.00	90.00	90.00	P2 ₁ 2 ₁ 2 ₁
81L	(FN ₂ C ₁₃) ₈	FN ₂ C ₁₃	8.45	9.94	24.20	90.00	90.00	90.00	Pbca
82LD	(OC ₃₀) ₈	OC ₃₀	44.05	10.69	8.89	90.00	90.00	90.00	Pbcn
83D	(OC ₄₆) ₈	(OC ₄₆) ₄	13.87	16.59	36.17	90.00	90.00	94.51	P-1
84	(OC ₅₂) ₈	(OC ₅₂) ₂	13.91	35.89	16.66	90.00	94.47	90.00	P2 ₁ /n
85	(C ₅₂) ₈	(C ₅₂) ₂	13.71	36.11	17.20	90.00	94.54	90.00	P2 ₁ /n
86	(O ₃ C ₂₉) ₈	O ₃ C ₂₉	22.04	24.62	7.85	90.00	90.00	90.00	Pccn
87	(BrOC ₅₂) ₄	(BrOC ₅₂) ₂	10.90	19.50	21.65	80.36	75.79	81.10	P-1
88	(BrOC ₅₂) ₄	(BrOC ₅₂) ₂	10.90	10.92	17.51	73.24	85.95	76.13	P-1

Sample	Cell content	Asymmetric unit	a(Å)	b(Å)	c(Å)	$\alpha(^{\circ})$	$\beta(^{\circ})$	$\gamma(^{\circ})$	space group
89	(C ₅₂) ₆	(C ₅₂) ₃	12.56	12.56	36.32	90.40	90.40	98.46	P-1
90	(ClO ₁₁ N ₇ C ₂₆) ₂	ClO ₁₁ N ₇ C ₂₆	8.95	12.19	14.88	83.86	75.60	80.45	P-1
91	(ClO ₅ N ₇ C ₂₆) ₂	ClO ₅ N ₇ C ₂₆	8.43	13.42	13.68	108.22	103.75	107.49	P-1
92	(PtO ₃ N ₅ C ₂₈) ₈	PtO ₃ N ₅ C ₂₈	23.32	14.45	22.39	90.00	115.22	90.00	Aba2
93	(ON ₃ C ₂₀) ₈	ON ₃ C ₂₀	29.91	4.99	25.88	90.00	125.14	90.00	C2/c
94	(ONC ₁₅) ₁₆	(ONC ₁₅) ₂	19.87	25.52	9.52	90.00	90.00	90.00	Pccn
95	(ON ₃ C ₁₆) ₄	ON ₃ C ₁₆	15.93	4.79	20.43	90.00	111.82	90.00	P2/c
96	(O ₂ C ₄) ₄	OC ₂	15.12	3.90	15.84	90.00	106.49	90.00	C2/c
97	(ON ₃ C ₂₁) ₈	ON ₃ C ₂₁	22.47	22.47	6.48	90.00	90.00	90.00	P4 ₂ /n
98	(O ₃ N ₃ C ₁₆) ₄	O ₃ N ₃ C ₁₆	15.89	4.78	20.36	90.00	111.87	90.00	P2/c
99	(SN ₂ C ₁₈) ₂	SN ₂ C ₁₈	6.96	9.00	12.25	92.74	95.60	106.98	P-1
100	(SO ₂ N ₂ C ₂₆) ₄	(SO ₂ N ₂ C ₂₆) ₂	12.17	13.18	14.58	91.76	107.65	98.31	P-1
101	(O ₃ N ₄ C ₂₈) ₄	O ₃ N ₄ C ₂₈	17.33	17.34	7.78	90.00	90.00	90.00	Pna2 ₁
102	(O ₃ N ₂ C ₂₁) ₄	(O ₃ N ₂ C ₂₁) ₄	9.57	11.84	16.03	89.98	90.10	90.04	P1
103	(ON ₃ C ₂₂) ₄	(ON ₃ C ₂₂) ₂	5.86	9.62	30.72	90.00	90.00	93.68	P-1
104	(PdS ₆ P ₄ C ₆₈) ₄	PdS ₆ P ₄ C ₆₈	23.32	14.45	22.39	90.00	115.22	90.00	P2 ₁ /c
105	(S ₄ O ₂ C ₂₀) ₂	S ₄ O ₂ C ₂₀	10.38	12.75	24.43	90.00	90.00	90.00	Pc
106	Fe ₃ Cl ₆ N ₂ C ₈₂	Fe _{3/2} Cl ₃ NC ₄₁	10.25	13.25	15.16	70.13	76.32	87.71	P-1
107	(P ₂ C ₂₆) ₄	P ₂ C ₂₆	12.76	12.99	14.07	90.00	116.69	90.00	P2 ₁ /c
108	(ReI ₃ S ₄ N ₂ C ₁₈) ₂	ReI ₃ S ₄ N ₂ C ₁₈	8.21	9.73	19.92	76.01	78.11	65.04	P-1
109	(OC ₁₅) ₄	OC ₁₅	4.14	13.99	17.12	90.00	90.00	90.00	P2 ₁ 2 ₁ 2 ₁
110	(O ₂ C ₃₀) ₂	O ₂ C ₃₀	9.54	10.79	11.20	74.42	65.97	76.35	P-1
111	(S ₄ P ₂ C ₁₆) ₄	S ₄ P ₂ C ₁₆	11.55	18.17	11.79	90.00	107.95	90.00	P2 ₁ /c
112	(BrC ₁₄) ₄	BrC ₁₄	3.97	13.99	18.33	90.00	95.94	90.00	P2 ₁ /c
113	(O ₂ C ₃₀) ₄	O ₂ C ₃₀	12.64	6.25	25.05	90.00	90.00	90.00	Pna2 ₁
114	(S ₂ NC ₁₃) ₄	S ₂ NC ₁₃	7.42	14.21	12.59	90.00	106.50	90.00	P2 ₁ /n
115	(BrC ₁₄) ₄	BrC ₁₄	3.97	14.00	18.33	90.00	95.95	90.00	P2 ₁ /c
116	(O ₂ NC ₇) ₂	O ₂ NC ₇	7.33	7.45	7.81	96.02	108.53	117.62	P-1
117	(BrO ₃ N ₃ C ₁₅) ₈	BrO ₃ N ₃ C ₁₅	25.97	10.55	12.38	90.00	101.24	90.00	C2/c
118	(BrO ₃ C ₁₁) ₄	BrO ₃ C ₁₁	7.09	14.39	10.04	90.00	90.00	90.00	Pna2 ₁
119	(SF ₃ O ₄ N ₂ C ₁₄) ₄	(SF ₃ O ₄ N ₂ C ₁₄) ₂	4.63	14.46	23.63	94.02	93.11	96.48	P-1
120	(O ₅ C ₁₃) ₈	O ₅ C ₁₃	8.22	13.87	20.84	90.00	96.06	90.00	C2/c
121	(I ₂ O ₂ NC ₁₄) ₈	I ₂ O ₂ NC ₁₄	37.75	4.52	17.33	90.00	116.74	90.00	C2/c
122	(I ₂ O ₄ NC ₁₆) ₄	I ₂ O ₄ NC ₁₆	7.91	14.70	14.07	90.00	90.00	90.00	Pca2 ₁
123	(BrOC ₅₀) ₂	BrOC ₅₀	12.97	13.06	13.41	70.14	82.72	60.48	P-1
124	(BrC ₁₃) ₄	BrC ₁₃	10.21	10.96	11.54	90	112.21	90	P2 ₁ /c
125	(ON ₂ C ₂₁) ₄	ON ₂ C ₂₁	10.31	11.60	12.15	90.00	99.04	90.00	Cc
126	(SO ₃ NC ₂₁) ₄	SO ₃ NC ₂₁	6.16	12.07	23.42	90.00	96.31	90.00	P2 ₁ /c
127	(SFO ₃ NC ₁₅) ₄	SFO ₃ NC ₁₅	11.83	8.29	14.16	90.00	102.81	90.00	P2 ₁ /c
128	(SO ₅ NC ₁₂) ₄	SO ₅ NC ₁₂	8.27	8.81	17.32	90.00	98.85	90.00	P2 ₁ /n
129	(SO ₅ NC ₁₂) ₄	SO ₅ NC ₁₂	8.27	8.81	17.33	90.00	98.83	90.00	P2 ₁ /n
130	(SCl ₂ O ₃ NC ₁₅) ₄	SCl ₂ O ₃ NC ₁₅	13.57	11.74	9.48	90.00	101.05	90.00	P2 ₁ /c
131	(SClO ₃ NC ₁₅) ₄	SClO ₃ NC ₁₅	13.38	11.17	9.77	90.00	98.65	90.00	P2 ₁ /c
132	(SClO ₃ NC ₁₅) ₄	SClO ₃ NC ₁₅	13.38	11.16	9.78	90.00	98.62	90.00	P2 ₁ /c

Sample	Cell content	Asymmetric unit	a(Å)	b(Å)	c(Å)	$\alpha(^{\circ})$	$\beta(^{\circ})$	$\gamma(^{\circ})$	space group
133	(SO ₃ NC ₁₆) ₄	(SO ₃ NC ₁₆) ₂	9.85	11.81	15.65	104.33	101.29	97.68	P-1
134	(SO ₃ NC ₂₁) ₄	SO ₃ NC ₂₁	5.98	12.06	25.18	90.00	90.00	90.00	P2 ₁ 2 ₁ 2 ₁
135	(SO ₅ NC ₁₁) ₄	SO ₅ NC ₁₁	12.67	7.75	12.97	90.00	95.86	90.00	P2 ₁ /n
136	(SO ₅ NC ₁₈) ₄	SO ₅ NC ₁₈	10.43	10.49	15.83	90.00	99.98	90.00	P2 ₁ /c
137	(SO ₅ NC ₁₇) ₈	(SO ₅ NC ₁₇) ₂	21.34	10.24	16.49	90.00	96.82	90.00	P2 ₁ /c
138	(SO ₅ NC ₁₇) ₈	(SO ₅ NC ₁₇) ₂	21.32	10.24	16.49	90.00	96.80	90.00	P2 ₁ /c
139	(SO ₃ NC ₁₇) ₈	(SO ₃ NC ₁₇) ₂	21.33	11.62	11.90	90.00	90.00	90.00	Pna2 ₁
140	(SO ₃ N ₃ C ₁₁) ₈	(SO ₃ N ₃ C ₁₁) ₂	26.39	10.45	9.02	90.00	96.33	90.00	P2 ₁ /c
141	(NiS ₄ C ₃₆) ₂	Ni _{1/2} S ₂ C ₁₈	8.44	14.09	13.59	90.00	96.15	90.00	P2 ₁ /c
142	(P ₂ C ₂₆) ₄	P ₂ C ₂₆	12.76	12.99	14.07	90.00	116.69	90.00	P2 ₁ /c
143	(Sn ₂ S ₈ N ₂ C ₁₈) ₄	Sn ₂ S ₈ N ₂ C ₁₈	18.98	9.70	16.74	90.00	111.68	90.00	P2 ₁ /c
144	(SnS ₂ N ₂ C ₆) ₄	SnS ₂ N ₂ C ₆	12.34	7.80	9.75	90.00	90.00	90.00	Pnmm
145	(S ₁₃ F ₃₆ N ₆ C ₃₀) ₂	S ₁₃ F ₃₆ N ₆ C ₃₀	12.09	12.40	20.28	75.84	75.22	88.40	P-1
146	(Se ₅ N ₂ C ₁₀) ₄	Se ₅ N ₂ C ₁₀	6.68	9.91	25.36	90.00	90.00	90.00	P-1
147	(Mo ₃ Se ₁₃ N ₃ C ₂₇) ₁₂	(Mo ₃ Se ₁₃ N ₃ C ₂₇) ₃	28.18	13.74	41.02	90.00	90.92	90.00	P2 ₁ /c
148	(O ₂ C ₁₆) ₄	(O ₂ C ₁₆) ₂	7.55	14.00	11.97	90.00	94.93	90.00	P2 ₁
149	(SO ₂ C ₁₁) ₄	SO ₂ C ₁₁	5.88	8.96	18.36	90.00	90.00	90.00	P2 ₁ 2 ₁ 2 ₁
150	(O ₃ C ₃₁) ₄	O ₃ C ₃₁	9.14	10.88	15.43	88.55	74.15	84.69	P-1
151	(Mo ₃ S ₁₂ N ₅ C ₃₉) ₄	(Mo ₃ S ₁₂ N ₅ C ₃₉) ₂	11.23	18.28	32.61	90.00	99.76	90.00	Pn
152	(Mo ₃ S ₁₂ ON ₅ C ₂₃) ₂	Mo ₃ S ₁₂ ON ₅ C ₂₃	10.61	11.40	19.04	87.49	80.55	69.72	P-1
153	(Mo ₃ BrS ₁₃ P ₆ N ₃ O ₁₈ C ₃₆) ₈	(Mo ₃ BrS ₁₃ P ₆ N ₃ O ₁₈ C ₃₆) ₂	33.69	12.51	36.59	90.00	98.76	90.00	P2 ₁ /n
154	(NiS ₄ C ₆₀) ₄	Ni _{1/2} S ₂ C ₃₀	25.70	14.67	19.27	90.00	116.92	90.00	C2/c
155	(Re ₂ Se ₄ O ₆ N ₂ C ₁₁) ₂	Re ₂ Se ₄ O ₆ N ₂ C ₁₁	11.46	10.70	12.45	84.76	81.72	63.17	P-1
156	(ON ₃ C ₁₁) ₄	ON ₃ C ₁₁	10.93	18.43	4.75	90.00	90.00	90.00	Pna2 ₁
157	(ClON ₄ C ₁₆) ₄	ClON ₄ C ₁₆	13.30	13.21	8.63	90.00	106.20	90.00	P2 ₁ /c
158	(O ₂ N ₄ C ₃₈) ₄	O ₂ N ₄ C ₃₈	17.36	10.89	17.92	90.00	117.32	90.00	P2 ₁ /c
159	(FO ₄ N ₃ C ₁₈) ₂	FO ₄ N ₃ C ₁₈	8.33	9.47	10.45	102.48	96.75	96.84	P-1
160	(O ₂ N ₄ C ₁₁) ₄	O ₂ N ₄ C ₁₁	10.89	9.25	11.71	90.00	115.35	90.00	P2 ₁ /c
161	(SO ₆ N ₂ C ₁₆) ₂	SO ₆ N ₂ C ₁₆	8.85	10.69	12.71	74.94	83.33	84.22	P-1
162	(ClSO ₄ NC ₁₆) ₈	ClSO ₄ NC ₁₆	9.57	15.01	21.98	90.00	90.00	90.00	Pbca
163	(SO ₄ NC ₁₇) ₄	(SO ₄ NC ₁₇) ₂	11.77	5.57	25.09	90.00	103.17	90.00	P2 ₁
164	(SO ₄ NC ₁₇) ₄	SO ₄ NC ₁₇	11.76	5.57	25.03	90.00	102.77	90.00	P2 ₁ /n
165	(SO ₄ NC ₁₇) ₄	SO ₄ NC ₁₇	11.76	5.57	25.03	90.00	102.73	90.00	P2 ₁ /n
166	(O ₅ C ₁₀) ₂	O ₅ C ₁₀	7.80	8.53	8.57	100.06	95.46	95.26	P-1
167	(O ₃ N ₂ C ₇) ₄	O ₃ N ₂ C ₇	16.04	6.40	7.16	90.00	90.00	90.00	Pnma
168	(ClSO ₄ NC ₂₁) ₄	ClSO ₄ NC ₂₁	8.07	19.00	13.93	90.00	92.33	90.00	P2 ₁ /n
169	(SO ₃ N ₅ C ₈) ₄	SO ₃ N ₅ C ₈	4.85	14.39	15.56	90.00	91.80	90.00	P2 ₁ /c
170	(SO ₅ N ₃ C ₂₄) ₄	SO ₅ N ₃ C ₂₄	9.17	19.63	13.02	90.00	91.01	90.00	P2 ₁ /n
171	(O ₂ N ₃ C ₂₅) ₄	O ₂ N ₃ C ₂₅	17.49	7.09	17.65	90.00	105.77	90.00	P2 ₁ /c
172	(ClO ₂ N ₄ C ₃₁) ₄	ClO ₂ N ₄ C ₃₁	12.86	4.54	15.68	90.00	106.67	90.00	P2 ₁ /n
173	(BrO ₂ N ₄ C ₃₃) ₄	BrO ₂ N ₄ C ₃₃	13.11	14.54	15.60	90.00	107.12	90.00	P2 ₁ /n
174	(SO ₃ NC ₆) ₄	SO ₃ NC ₆	9.49	6.92	11.72	90.00	103.29	90.00	P2 ₁ /c
175	(SO ₅ N ₃ C ₂₀) ₂	SO ₅ N ₃ C ₂₀	8.19	9.96	12.59	89.22	81.73	75.95	P-1
176	(Cl ₂ SO ₄ N ₃ C ₂₃) ₄	Cl ₂ SO ₄ N ₃ C ₂₃	9.17	20.25	13.12	90.00	91.34	90.00	P2 ₁ /n

Sample	Cell content	Asymmetric unit	a(Å)	b(Å)	c(Å)	$\alpha(^{\circ})$	$\beta(^{\circ})$	$\gamma(^{\circ})$	space group
177	(SO ₅ N ₄ C ₁₈) ₈	(SO ₅ N ₄ C ₁₈) ₄	8.13	16.27	28.38	93.20	93.14	102.09	P-1
178	(SO ₂ N ₂ C ₁₈) ₂	SO ₂ N ₂ C ₁₈	6.87	9.26	13.88	106.35	93.10	107.42	P-1
179	(Cl ₂ SO ₄ N ₂ C ₁₆) ₄	Cl ₂ SO ₄ N ₂ C ₁₆	8.14	9.35	22.27	90.00	96.38	90.00	P2 ₁ /n
180	(S ₄ O ₈ N ₆ C ₃₈) ₂	S ₄ O ₈ N ₆ C ₃₈	8.24	15.04	15.87	101.68	104.67	98.86	P-1
181	(S ₂ O ₅ N ₃ C ₁₉) ₄	S ₂ O ₅ N ₃ C ₁₉	7.53	12.47	20.54	90.00	92.47	90.00	P2 ₁ /c
182	(ClN ₂ C ₁₃) ₈	ClN ₂ C ₁₃	9.16	9.74	26.63	90.00	90.00	90.00	Pbca
183	(O ₂ N ₅ C ₂₀) ₂	O ₂ N ₅ C ₂₀	5.50	10.29	15.81	87.68	88.89	79.39	P-1
184	(N ₂ C ₂₀) ₄	N ₂ C ₂₀	5.95	16.89	15.09	90.00	90.66	90.00	P2 ₁ /c
185	(CuCl ₄ NaN ₂ C ₁₃) ₄	(CuCl ₄ NaN ₂ C ₁₃) ₂	7.59	7.00	30.47	90.00	90.91	90.00	P2 ₁
186	(O ₅ N ₂ C ₂₂) ₄	O ₅ N ₂ C ₂₂	11.52	7.42	22.24	90.00	91.81	90.00	P2 ₁ /n
187	(O ₂ N ₅ C ₂₀) ₂	O ₂ N ₅ C ₂₀	5.50	10.29	15.80	87.65	88.93	79.35	P-1
188	(BrOC ₅₂) ₂	BrOC ₅₂	12.97	13.06	13.42	70.18	82.71	60.50	P-1
189	(Cl ₄ O ₂ C ₂₈) ₄	Cl ₄ O ₂ C ₂₈	17.99	7.40	18.48	90.00	118.24	90.00	P2 ₁ /n
190	(O ₄ N ₂ C ₁₆) ₄	O ₄ N ₂ C ₁₆	11.58	7.49	16.72	90.00	94.19	90.00	P2 ₁ /c
191	(BrO ₃ N ₃ C ₁₅) ₂	BrO ₃ N ₃ C ₁₅	16.11	5.80	7.43	90.00	94.74	90.00	Pc
192	(O ₅ C ₁₂) ₄	O ₅ C ₁₂	8.88	18.17	7.72	90.00	106.04	90.00	Cc
193	(O ₃ N ₄ C ₂₇) ₄	O ₃ N ₄ C ₂₇	17.33	17.34	7.78	90.00	90.00	90.00	Pna2 ₁
194	(S ₂ O ₃ C ₁₃) ₄	S ₂ O ₃ C ₁₃	11.43	7.93	16.78	90.00	108.78	90.00	P2 ₁ /c
195	(O ₃ N ₂ C ₂₁) ₄	O ₃ N ₂ C ₂₁	9.56	16.03	11.84	90.00	90.00	90.00	Pca2 ₁
196	(ON ₃ C ₂₂) ₄	ON ₃ C ₂₂	14.22	5.58	22.06	90.00	93.44	90.00	P2 ₁ /n
197	(S ₂ ON ₅ C ₁₈) ₄	S ₂ ON ₅ C ₁₈	14.77	7.35	17.98	90.00	106.96	90.00	P2 ₁ /n
198	(ON ₃ C ₂₂) ₄	(ON ₃ C ₂₂) ₂	9.62	30.72	5.86	90.00	93.68	90.00	P2 ₁ /c
199	(ON ₃ C ₂₂) ₄	ON ₃ C ₂₂	14.23	5.59	22.07	90.00	93.90	90.00	P2 ₁ /n
200	(O ₂ N ₄ C ₁₅) ₂	O ₂ N ₄ C ₁₅	16.12	5.80	7.43	90.00	94.75	90.00	Pc
201	(O ₅ N ₄ C ₁₄) ₄	O ₅ N ₄ C ₁₃	5.52	17.79	15.69	90.00	91.62	90.00	P2 ₁ /n
202	(O ₂ N ₅ C ₁₃) ₄	O ₂ N ₅ C ₁₃	9.34	9.28	16.52	90.00	97.74	90.00	P2 ₁ /n
203	(O ₅ N ₄ C ₁₄) ₄	O ₅ N ₄ C ₁₄	5.52	17.79	15.70	90.00	91.60	90.00	P2 ₁ /n
204	(O ₂ N ₂ C ₁₅) ₂	O ₂ N ₂ C ₁₅	7.53	8.56	10.74	75.50	84.28	84.83	P-1
205	(O ₄ N ₄ C ₁₆) ₄	O ₄ N ₄ C ₁₆	5.52	17.78	15.69	90.00	91.60	90.00	P2 ₁ /n
206	(O ₅ N ₄ C ₁₄) ₄	AgCl ₂ Si ₂ OC ₃₆	19.55	15.89	20.15	90.00	90.00	90.00	Pbca
207	(S ₂ N ₂ C ₂₆) ₄	S ₂ N ₂ C ₂₆	15.75	9.37	15.77	90.00	113.35	90.00	P2 ₁ /n
208	(ON ₃ C ₁₁) ₄	ON ₃ C ₁₁	10.42	5.31	16.06	90.00	95.26	90.00	P2 ₁ /n
209	(Cl ₂ O ₃ N ₂ C ₁₇) ₂	Cl ₂ O ₃ N ₂ C ₁₇	7.49	9.13	12.43	92.37	91.85	99.09	P-1
210	(O ₄ N ₂ C ₈) ₄	O ₄ N ₂ C ₈	6.91	13.10	10.45	90.00	106.79	90.00	P2 ₁ /c
211	(ON ₄ C ₂₀) ₄	ON ₄ C ₂₀	7.99	13.45	14.45	90.00	93.30	90.00	P2 ₁ /n
212	(Cl ₂ O ₃ N ₂ C ₁₇) ₂	Cl ₂ O ₃ N ₂ C ₁₇	7.50	9.14	12.43	92.33	91.92	99.06	P-1
213	(ClO ₃ N ₄ C ₂₂) ₂	ClO ₃ N ₄ C ₂₂	8.47	11.08	12.15	91.89	103.97	111.48	P-1
214	(O ₂ N ₅ C ₂₃) ₁₆	O ₂ N ₅ C ₂₃	26.08	26.08	16.04	90.00	90.00	90.00	I4 ₁ /a
215	(ON ₅ C ₁₇) ₄	(ON ₅ C ₁₇) ₂	8.91	12.80	13.86	94.25	98.37	101.40	P-1
216	(ON ₄ C ₂₁) ₄	ON ₄ C ₂₁	32.00	9.25	6.46	90.00	90.00	90.00	Pna2 ₁
217	(O ₄ N ₆ C ₂₀) ₄	O ₄ N ₆ C ₂₀	9.16	15.22	14.66	90.00	96.26	90.00	P2 ₁ /n
218	(O ₄ N ₅ C ₂₂) ₂	O ₄ N ₅ C ₂₂	8.38	10.65	12.96	79.16	83.90	67.81	P-1
219	(O ₆ N ₅ C ₂₅) ₂	O ₆ N ₅ C ₂₅	9.18	12.03	12.06	82.37	87.42	79.50	P-1
220	(O ₃ N ₅ C ₁₈) ₄	O ₃ N ₅ C ₁₈	16.21	16.21	14.30	90.00	90.00	90.00	P4 ₂ /n

Sample	Cell content	Asymmetric unit	a(Å)	b(Å)	c(Å)	α (°)	β (°)	γ (°)	space group
221	(O ₃ N ₃ C ₁₆) ₂	O ₃ N ₃ C ₁₆	9.14	9.49	10.01	79.55	63.79	83.05	P-1
222	(ClO ₃ N ₄ C ₂₁) ₄	ClO ₃ N ₄ C ₂₁	7.53	15.97	16.54	90.00	90.00	90.00	P2 ₁ 2 ₁ 2 ₁
223	(ON ₅ C ₁₉) ₄	ON ₅ C ₁₉	9.11	13.89	13.46	90.00	103.91	90.00	P2 ₁ /c
224	(O ₂ N ₅ C ₂₅) ₄	O ₂ N ₅ C ₂₅	11.31	9.46	21.56	90.00	94.27	90.00	P2 ₁ /n

References

Sheldrick, G. M. (2015a). *Acta Cryst.* **C71**, 3-8.

Sheldrick, G. M. (2015b). *Acta Cryst.* **A71**, 3-8.

Spek, A.L. (2020). *Acta Cryst.* **E76**, 1-11.

Yamano, A., Heo, N. H. & Teeter, M. M. (1997). *J Biol Chem.* **272**, 9597-9600.

Zhang, X. & Donahue, J. P. (2024). *Acta Cryst.* **A80**, 237-248.